THE JOURNAL OF BIOLOGICAL CHEMISTRY VOL. 287, NO. 41, pp. 34514–34532, October 5, 2012

The Antibodies against the Computationally Designed Mimic of the Glycoprotein Hormone Receptor Transmembrane Domain Provide Insights into Receptor Activation and Suppress the Constitutively Activated Receptor Mutants*[S]

Received for publication, February 21, 2012, and in revised form, August 16, 2012 Published, JBC Papers in Press, August 17, 2012, DOI 10.1074/jbc.M112.355032

Ritankar Majumdar, Reema Railkar[1], and Rajan R. Dighe[2]

From the Department of Molecular Reproduction, Development and Genetics, Indian Institute of Science, Bangalore 560012, India

Background: The mechanism of glycoprotein hormone receptor activation is not clearly understood.
Results: Antibodies against computationally designed TMD mimic bind TSHR/LHR/FSHR and inhibit hormone-independent and -dependent receptor activation without affecting respective hormone binding.
Conclusion: Conformational alterations in transmembrane helices leading to receptor activation are dependent on changes in hinge-exoloop engagements.
Significance: Antibodies against novel TMD mimic have therapeutic potential against gain-of-function diseases and provide insights into receptor activation.

The exoloops of glycoprotein hormone receptors (GpHRs) transduce the signal generated by the ligand-ectodomain interactions to the transmembrane helices either through direct hormonal contact and/or by modulating the interdomain interactions between the hinge region (HinR) and the transmembrane domain (TMD). The ligand-induced conformational alterations in the HinRs and the interhelical loops of luteinizing hormone receptor/follicle stimulating hormone receptor/thyroid stimulating hormone receptor were mapped using exoloop-specific antibodies generated against a mini-TMD protein designed to mimic the native exoloop conformations that were created by joining the thyroid stimulating hormone receptor exoloops constrained through helical tethers and library-derived linkers. The antibody against the mini-TMD specifically recognized all three GpHRs and inhibited the basal and hormone-stimulated cAMP production without affecting hormone binding. Interestingly, binding of the antibody to all three receptors was abolished by prior incubation of the receptors with the respective hormones, suggesting that the exoloops are buried in the hormone-receptor complexes. The antibody also suppressed the high basal activities of gain-of-function mutations in the HinRs, exoloops, and TMDs such as those involved in precocious puberty and thyroid toxic adenomas. Using the antibody and point/deletion/chimeric receptor mutants, we demonstrate that changes in the HinR-exoloop interactions play an important role in receptor activation. Computational analysis suggests that the mini-TMD antibodies act by conformationally locking the transmembrane helices by means of restraining the exoloops and the juxta-membrane regions. Using GpHRs as a model, we describe a novel computational approach of generating soluble TMD mimics that can be used to explain the role of exoloops during receptor activation and their interplay with TMDs.

The class A rhodopsin type receptors form the largest subset of the G protein-coupled receptor superfamily bearing the canonical heptahelical serpentine domain and a common mode of activation through the heterotrimeric G-proteins. The ligand binding sites in these receptors primarily lie buried inside transmembrane helices (TMH)[3] (opsin, odorant receptors) or in the juxta-membrane regions (neuropeptides, small endogenous ligands) (1), with the notable exception of the glycoprotein hormone receptor (GpHR) family comprising the thyroid stimulating hormone receptor (TSHR), follicle-stimulating hormone receptor (FSHR), and luteinizing hormone (LH) receptor (LHR). The specific binding of the respective ligands, thyroid stimulating hormone (TSH), follicle-stimulating hormone (FSH), and LH/human chorionic gonadotropin (hCG), to these receptors takes place at the large extracellular domains (ECD)-containing tandem repeats of nine or more leucine-rich repeats (LRR) flanked by the cysteine box (Cb) motifs (2), and the signals thus generated are transmitted to the distally situated transmembrane domains (TMD), a process still not well understood.

Various models have been proposed to explain the mechanism of signal transmission between these two distinct regions. A model for receptor activation, mainly derived directly from

* This work was supported by grants from the Department of Biotechnology, Government of India, New Delhi.
[S] This article contains supplemental Fig. 1.
[1] Recipient of a Council of Scientific and Industrial Research, New Delhi, fellowship.
[2] To whom correspondence should be addressed. Tel.: 91-080-22933261; Fax: 91-080-23600999; E-mail: rdighe@mrdg.iisc.ernet.in.

[3] The abbreviations used are: TMH, transmembrane helix; hCG, human chorionic gonadotropin; FSH, follicle stimulating hormone; FSHR, FSH receptor; TSH, thyroid stimulating hormone, TSHR, TSH receptor; LH, luteinizing hormone; LHR, LH receptor; GpHR, glycoprotein hormone receptor; ECD, extracellular domain; LRR, leucine-rich repeat; ECL, extracellular loop; ICL, intracellular Loops; CAM, constitutively activating mutation; Cb-2/3, cysteine box-2/3; NRIgG, normal rabbit IgG (pre-immune); MD, molecular dynamics; r.m.s.d., root mean square deviation; Ni^{+2}-NTA, nickel-nitrilotriacetic acid; aa, amino acid; TMD, transmembrane domain; HinR, hinge region; RMFI, relative mean fluorescence intensity; Ra, relative accessibility; Re, relative surface expression.

the crystal structure of FSH-FSHR ECD, suggests receptor activation occurs through direct interactions of the loops 1 and 3 of the common α-subunit of the hormones with the TMD and the extracellular loops (ECL) after the determinant loops of the β subunits of hormones make initial contacts with the LRRs (2). This model of receptor activation has been challenged by Moyle *et al.* (3), who envisaged additional contacts between the ECD and ECLs to be critical for receptor activation. These multipoint interactions are thought to occur between the N-terminal ECD and the ECLs through the β-loop region of the LRR. On the contrary, it has also been reported that the C-terminal region of the ECD makes extensive contacts with the ECLs 1 and 2 and lies parallel to the concave surface of the LRR domain (4). Difficulty in ascertaining the correct model stems from the unavailability of the structural information on the C-terminal region of the ECD called the hinge region (HinR). Initially thought to be a structural scaffold, HinR was assumed to act as a flexible hinge facilitating contacts between the hormone and the TMD (5). However, the recent mutation-based evidence (6) and our earlier studies on the agonistic antibodies against the FSHR HinR (7) suggest that the HinR may be involved in hormone-dependent as well as independent activation of the receptor. Moreover, the presence of activating mutations at the conserved motifs in the cysteine box-2/3 (Cb-2/3) of HinR and the combined effect of such mutations with those present in the exoloops have helped in development of an alternate model of receptor activation where the HinR acts as a "tethered inverse agonist" constraining the receptor in an inactive state which is reversed by hormone binding resulting in its activation (8).

A major difficulty in deriving a holistic view of the receptor activation process is the inability to demonstrate direct interactions between the hormone and the ECLs and/or HinR. Moreover, the models do not take into account unique attributes of each member of GpHR family such as the relatively higher basal cAMP production of TSHR compared with LHR or FSHR and the variations in interactions between each receptor component. Although the cooperativity between ECLs during receptor activation is well documented (9), role of individual loops or change in their spatio-geometric arrangement during receptor activation is not clearly understood. Mutational studies provide only transitional information on these highly dynamic interactions.

Antibodies are the ideal tools to monitor such activation-related conformational changes during ligand-receptor interaction. For example, the ability of ECL-specific antibodies of rhodopsin (10) and CCR5 receptors (11) to distinguish between the conformations of the loops in inactive and active states of the receptors highlights their suitability to study the ECLs of GpHRs. Unfortunately, there have not been many reports on antibodies against the exoloops of GpHRs that recognize the native conformations of the loops as they exist in the wild type receptor. Inherent difficulties in obtaining soluble TMDs for raising antibodies and loss of conformational information in the ECL peptide-specific antibodies are the primary causes of such lacunae.

We have, therefore, used a novel approach of designing a recombinant mini-TMD protein where TSHR ECLs are computationally joined to intracellular loops (ICLs) through the library-derived linkers and helical tethers, thus preserving the natural spatio-geometric arrangement of the ECLs in the native TMD of the receptor. This approach circumvents the difficulties in generation of a soluble TMD while maintaining the relative arrangements of the ECLs with respect to each other. Binding and functional studies with antibodies against such a protein provide novel insights into the role of ECLs in GpHR activation.

EXPERIMENTAL PROCEDURES

Modeling of the Transmembrane Domain—A bipartite strategy was employed to model TMDs, the first step being to model the individual helices and loops and then create a composite model by joining ECLs/ICLs with the modeled TMH. The scheme of the strategy used is shown in supplemental Fig. S1.

A multitemplate approach was employed to model (using Modeler 9.07 (12)) the individual helices of TSHR TMD to incorporate structural features of G protein-coupled receptors that are distributed over different crystal structures and may not be represented by a single template (13). The human β2-adrenergic receptor (PDB ID 2RH1) served as the optimum template for TMHs 2, 3, and 6 as it conforms to the absence of the glycine bend or disulfide bridge in the helix 2 the absence of a second disulfide bridge between TMH6 and ECL3 and an insertion in TMH3. The turkey β1 adrenergic receptor (PDB ID 2VT4) was the template of choice for TMH1 due to the absence of glycine-glycine or proline motifs, whereas the squid rhodopsin (PDB ID 2Z73) was used for modeling TMH4 and TMH7. Bovine rhodopsin (PDB ID 1U19), similar to TSHR, does not contain an intra ECL2 disulfide bridge with TMH5 and hence was used as a template for modeling the same. A regular helix extension was carried out for TMH2 and TMH5 in the absence of the characteristic structural bulges caused by consecutive threonines in TMH2 or proline in TMH5 of squid rhodopsin.

Rotational and translational symmetry operations on the modeled TMH were carried out to simulate a membrane-bound G protein-coupled receptor by implicitly adding a 30 Å membrane and setting shift angles to 15° from −6° to +9° and rotation to −50°. The structural alignments of the modeled TMHs and their respective templates are shown in Fig. 1*A*.

The ECLs and the ICLs were modeled by first searching the database of Loops In Membrane Proteins (LIMP) (14) for loops with sequences and gap tolerance similar to the beginning and ends of each TMH. These candidate loops were joined to the modeled TMH by a loop-closing algorithm implemented in cyclic coordinate descent (CCD) module of Rosetta 3.1 (15), and the loop conformations were optimized by systematic conformational sampling of the loop backbone followed by energy minimization (16). Several TSHR-specific loop constraints were implemented during loop optimization. First, the β-sheet-like hairpin structure of ECL2 was maintained between the transmembrane helices based on the rhodopsin structure and those proposed in the case of the CCR5 chemokine receptor (17). Second, the ICL3 conformations were adopted from the NMR structure of the rhodopsin cytosolic loop peptide complex (18), and last, the placement of ECLs 1 and 3 at TMH periphery was carried out according to the previously reported mutational data (9).

Molecular Dynamics (MD) simulations were performed on the composite model of TSHR TMH and ECLs/ICLs after being typed with implicit membrane solvation under the CHARMm27 force field (INSIGHTII 2000 (20)). The solvent in each minimized system was equilibrated for 10 ps while gradually heating the model from 0 to 300 K in 25 ps followed by a second equilibrium phase of 25 ps under a constant pressure and finally subjected to a 1-ns isothermal, constant volume MD simulations. Additional restrain parameters such as a disulfide bridge patch between residues Cys-494 and Cys-569 were applied during MD simulations, and the distance restraints were imposed for maintenance of the α-helical regions in TMD. A similar procedure was also adopted for modeling the transmembrane domains of LHR.

Rationale, Design, Assembly, Expression, and Purification of the Mini-TMD Protein—The mini-TMD protein was synthetically created by joining the ECLs to the ICLs by tethering them with the juxtamembrane elements adjacent to the membrane interface as shown in Fig. 1*B*. The ECL1 (Ser-479–Thr-490) was connected to ECL2 (Gly-559–Pro-577) using the ICL2 (Thr-524–Ile-533) as the linker. Ala-471–His-478, part of the TMH2, was used to tether the N terminus of the ECL1, whereas the first three residues of TMH 3 (Pro-492–Cys-494) were joined to the last two residues of TMH3 (Trp-520–Tyr-521) to connect the ECL1 to the ICL2. The ICL2 was in turn connected to the ECL2 by helix elements formed by the first five residues (Arg-534–Ala-538) and the last six residues (Ala-553–Val-558) of the TMH4. The ECL2 was similarly connected to the ECL3 (Asn-650–Ser-657) using the ICL3 (Val-608–Asp-617) as a linker where the helix segments in the TMH5 (Ala–579–Val-584) acted as the N-terminal tether, whereas Ala-647–Asn-650 in the TMH6 acted as the C-terminal tether. The helix element in the TMH 7 (Ser-659–Val-664) was used to stabilize the C-terminal end of the mini-TMD. The optimum length of the above-mentioned helical tethers used for joining ECLs to ICLs was determined by growing the helical chain by successive addition of N-terminal and C-terminal residues of the helical segment and concomitant prediction of the secondary structure conformation using iterative Tasser simulations (21).

The assembled sequence was modeled on the energy-minimized TSHR TMD structure to identify the regions of distorted geometry and potential steric clashes. Dihedral violations were observed at Ile-26 corresponding to the residue Ile-523 belonging to the C-terminal tether of ECL2. Helix discontinuity was also observed for Ala-522 and Thr-524 in the same region. An *in silico* mutagenic scan was undertaken for these two residues that would enable regular helix extension in this region, and based on these scans, both residues were replaced by threonine and alanine, respectively. The main chain bond angle violations were also observed for Leu-578 where an extended coil was noticed in place of the expected β-turn. This might arise due to the presence of proline (Pro-577) in the PLA motif, and a search of the precomputed secondary structure assignments for different crystal structures (22) revealed that substituting Leu-578 with glycine may restore the correct secondary structure.

The corrected mini-TMD protein sequence was reverse-translated to obtain the encoding DNA sequence which was codon-optimized for expression in *Escherichia coli*. The resultant sequence was synthetically assembled by a modified two-step multiplex PCR (23) where the multiple overlapping primers yielded an amplified mixture of annealing combinations. This mixture was subsequently used as the template for assembling the entire full-length gene by the primers specific for the 5′ and 3′ ends corresponding to the N-terminal and the C-terminal regions of the designed protein, respectively. The mini-TMD encoding sequence was cloned into pPROexHtA vector and expressed in *E. coli* as a His-tagged protein and purified using nickel-nitrilotriacetic acid chromatography under native conditions.

Circular Dichroism Spectra of the Mini-TMD Protein—Circular Dichroism (CD) spectra of the mini TMD were recorded between 195 and 250 nm using the Jasco J810 polarimeter at the protein concentration of 10 μM at 25 °C in 10 mM phosphate buffer, pH 7.4, with the scan setting set to 1 nM wavelength pitch, 10 nm/min scanning speed in continuous mode, and 3 accumulations per measurement. The protein was reduced with 1 mM DTT and 20 μM 2-mercaptoethanol for 3 h, the CD spectra were recorded again, and the background was subtracted from observed ellipticities and converted into mean molar ellipticity per residue. The relative secondary structures were calculated using SELCON3, CDSSTR, and CONTINLL included in the CDpro spectra analysis package using a reference set of 43 proteins. A weighted average of the outputs of the three programs was considered reliable for estimating the secondary structure content of the protein.

TSHR/LHR/FSHR Wild Type and Mutant Constructs—Stable cell lines expressing WT TSHR, LHR, and FSHR were created in HEK293 background and characterized as described previously (7, 24, 25).

LRR- and ECD-deleted mutants and the activating mutations of TSHR and LHR used in the this study were created as described earlier for FSHR (7). Briefly, modified pcDNA3.1-MycHis vectors (Invitrogen) were created containing the signal peptides of TSHR/LHR/FSHR (pCDNA3.1-SP) and the DNA fragments encoding the receptors without their LRRs (TSHR HinTMD, aa 261–764; LHR HinTMD, aa 265–699; FSHR HinTMD, aa 260–695) and without their entire ECDs (TSHR TMD, aa 414–764; LHR TMD, aa 355–699; FSHR TMD, aa 367–695) of GpHRs were cloned downstream of the respective cognate signal peptides to ensure proper translocation to the cell surface.

The hinge region activating mutations S281I, gain-of-function mutation in TSHR ECL 1/2/3-I486T, -I568F, and -V656F, and the inactivating mutation D410N were introduced into TSHR wild type background using a two-step PCR-based mutagenesis (26). The LHR hinge region mutation S277Q corresponding to the TSHR S281I mutant and the activating mutations in the LHR TMD at TMH6 (D578Y) were similarly created.

The TSHR/LHR chimeric receptor (TSH-LHR-6) and the LHR TMH3 activating mutant, L457R, were kind gifts of Profs. Basil Rapoport (Cedars-Sinai Medical Center, UCLA) and Deborah Segaloff (University of Iowa, USA), respectively.

Generation and Characterization of the Mini-TMD Antibodies—Antibodies against the mini-TMD protein were generated as described earlier (27). Briefly, the protein (500 μg) emul-

sified with Freund's complete adjuvant was administered to adult rabbit subcutaneously at multiple sites. The treatment was repeated 21 days later followed by another injection in Freund's incomplete adjuvant after another 21 days. The subsequent saline boosters (200 μg) were administered at intervals of 30 days, and the animals were bled after 10 days. IgGs were purified from the antisera using protein G chromatography. The antibodies, referred to hereafter as the mini-TMD antibodies, were characterized for specific binding to its cognate antigen fragment in ELISA and to all three GpHRs using immunoblotting and flow cytometry.

Transfection Experiments—HEK293 cells seeded into 6-well ($\sim 10^6$ cells/well/2 ml), 24-well ($\sim 3 \times 10^5$ cells/well/500 μl), or 48-well ($\sim 10^5$ cells/well/250 μl) plates were transiently transfected with WT or mutated GpHR constructs (3.2 μg of the plasmid DNA/ml of the plating medium) using Lipofectamine 2000 reagent as per the manufacturer's protocol (Invitrogen), and the transgene expression studies were carried out 48 h later. In each experiment parallel plates were transfected simultaneously to determine the ligand binding to the intact cells and membrane preparations, flow cytometric analysis, and cAMP production as described elsewhere (24).

Receptor Binding and in Vitro Response—Binding characteristics of the WT and mutant receptors were investigated as described earlier (7). Briefly, the membrane preparations obtained from the cell lines expressing TSHR/LHR/FSHR ($\sim$50 μg/ml) were incubated with respective radioiodinated hormones ($\sim$ 0.14 nM ^{125}I-labeled hormone, specific activity of the tracer $\sim$ 0.26 μCi/fmol) at 37 °C for 1 h in a reaction volume of 200 μl. At the end of the incubation, PEG8000 was added (final concentration 2.5%) at 4 °C, and the hormone-receptor complex was separated by centrifugation at 5000 $\times$ *g* for 20 min and the supernatant discarded. The pellet was counted for radioactivity in the PerkinElmer Life Sciences γ-counter. The nonspecific binding was determined by adding excess unlabeled hormone (0.5 μg/tube). Each binding experiment was carried out in duplicate and repeated at least two times.

Whenever the effect of antibodies on hormone-receptor interactions was investigated, the receptor preparations were preincubated first with different concentrations of the antibodies for 1 h at 37 °C followed by the addition of the labeled hormone and continued incubation for one more hour. The bound hormone-receptor complex was determined as described above.

Similarly, to determine the effect of antibodies on hormone response, 10^5 cells/well (stable cell line or transiently transfected) were plated in a 48-well plate and 24 h later incubated with fresh medium containing 1 mM phosphodiesterase inhibitor, 3-isobutyl-1-methylxanthine for 30 min at 37 °C (100 μl) followed by incubation with the mini-TMD antibodies or preimmune IgG (NRIgG) for 1 h and finally with fixed or increasing concentrations of the hormones for 15 min at 37 °C (100 μl), and cAMP produced was determined by RIA (28). The effect of antibodies on hormone-independent receptor activation was investigated by omitting the hormones.

Flow Cytometric Analysis of Receptor Mutants—Flow cytometric analysis was performed to quantify the cell-surface expression of different receptor mutants and measure the relative accessibility of ECLs to the mini-TMD antibodies using the protocol described previously (24, 25). Briefly, HEK293 cells (approximately, 5×10^5) transfected with different GpHR constructs were detached by treatments with Ca^{+2}/Mg^{+2}-free PBS containing 1 mM EDTA and EGTA and washed with PBS followed by incubation with the mini-TMD antibodies or NRIgG in PBS containing 5% FBS on ice for 1 h. The cells were washed twice with the same buffer and incubated on ice for 1 h with a 1:500 dilution of FITC-conjugated secondary antibody (Sigma), and the cell surface binding of the antibodies was assessed using the FACSCANTO II (BD Biosciences) flow cytometer. The ratio of the normalized binding of the control antibody (specific against either LRRs or the HinR) to the WT receptor (relative mean fluorescence intensity-WT ($RMFI_{WT}$)) and the mutant (relative mean fluorescence intensity-mutant ($RMFI_{MUT}$)) indicates the relative cell surface expression of a given mutant (R*e*). A similar ratio determined using the mini-TMD antibodies instead of the control antibody provided information on the relative accessibility (R_a) of ECLs in receptor mutants and allowed comparison of mini-TMD antibody binding across different mutants.

RESULTS

Molecular Modeling of TSHR TMD and the Mini-TMD Proteins

TMD—The templates used in modeling of TSHR transmembrane helices have been mostly derived from the crystal structures in the inactive state of the receptors. For example, the Turkey β2-adrenergic receptor (β-AR) that served as a template for TMH1 was crystallized with the antagonist cyanopindolol (PDB ID 2VT4), whereas the crystal structure of human β-AR (PDB ID 2RH1) complexed with the inverse agonist carazolol served as the template for TMHs 2, -3, and -6. Similarly, the squid rhodopsin crystallized in its 11-*cis* conformation representing the receptor in the basal state (PDB ID 2Z73) served as the template for TMHs 4 and 7. Therefore, the TMD model derived from these templates can be assumed to represent the inactive "off" state of the receptor. The resting state of TSHR can be further corroborated by stabilization of both potential and total energy profiles of the modeled TSHR TMD in the first 50 ps of MD. Moreover, the presence of an ionic lock between R3.50 (*Ballesteros* Weinstein numbering, aa:Asn-519 in TSHR, aa:Arg-464 in LHR) in the highly conserved (E/D)RY motif in TMH3 and D6.30 at the Asp/Glu motif at the cytoplasmic face of TMH6 (TSHR aa:Asp-619, hLHR aa:Asp-564) indicates attainment of a minimized structure with intact functional interhelical interactions (Fig. 1*C*). Despite high variability of the extra/intracellular loops of TSHR, the signature sequence matched well with the previous mutational studies indicating reliable modeling. For example, the residues such as Lys-660 that have been proposed to be a toggle switch between the activated and inactive states through their interaction with ECL2 makes multiple ionic interactions with Asp-573 in ECL2, further validating the modeling procedure (30). However, the receptor-specific attributes were also noticed in the residues of the juxtamembrane region such as TSHR Tyr-643 that depicted a 12° turn toward ECL3 as compared with a phenylalanine at a similar position for LHR.

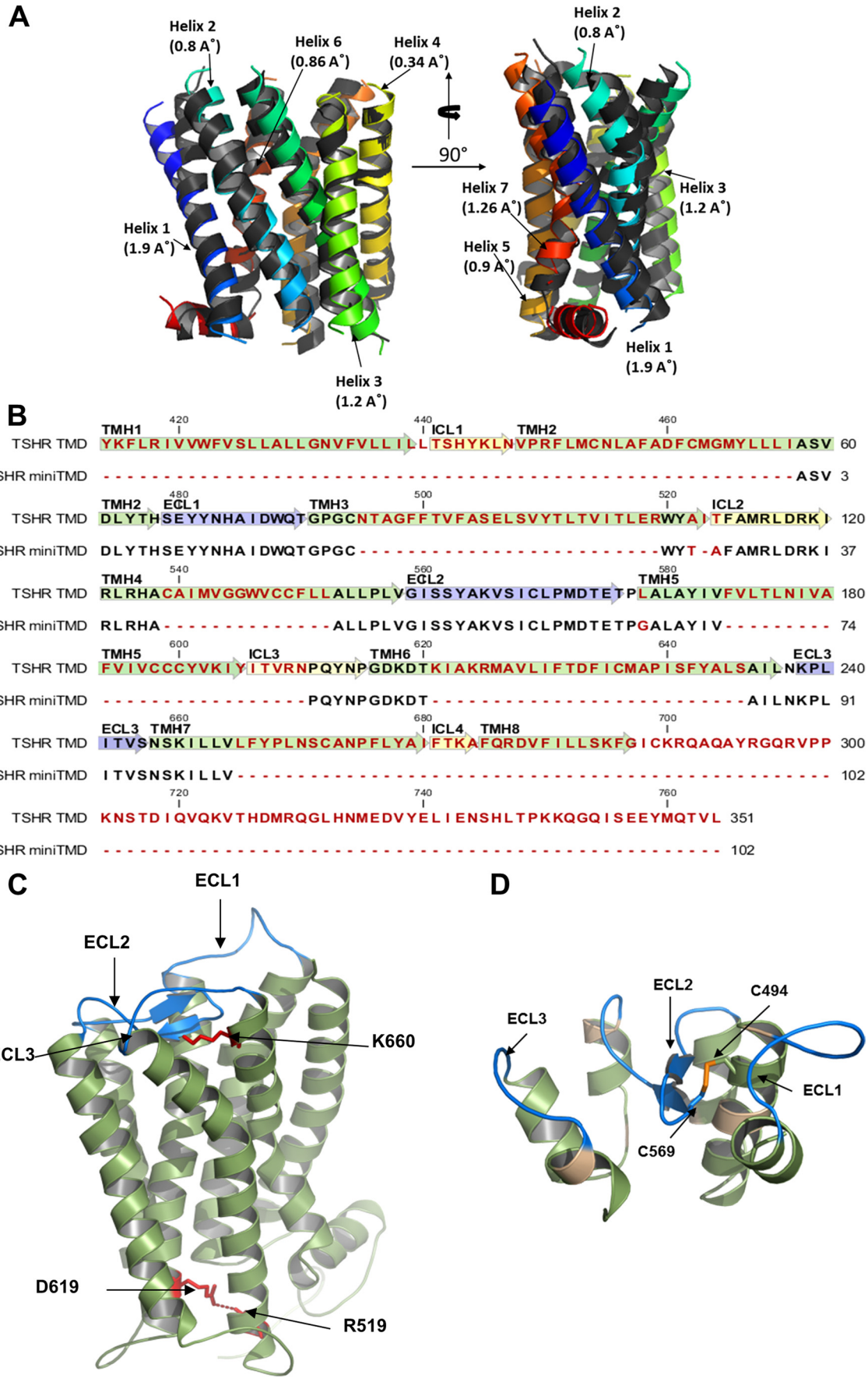
A
Helix 2 (0.8 A˚)
Helix 6 (0.86 A˚)
Helix 4 (0.34 A˚)
Helix 1 (1.9 A˚)
Helix 3 (1.2 A˚)
90°
Helix 2 (0.8 A˚)
Helix 7 (1.26 A˚)
Helix 3 (1.2 A˚)
Helix 5 (0.9 A˚)
Helix 1 (1.9 A˚)
B
TMH1 ICL1 TMH2
TSHR TMD YKFLRIVVWFVSLLALLGNVFVLLILLTSHYKLNVPRFLMCNLAFADFCMGMYLLLIASV 60
TSHR miniTMD ASV 3
TMH2 ECL1 TMH3 ICL2
TSHR TMD DLYTHSEYYNHAIDWQTGPGCNTAGFFTVFASELSVYTLTVITLERWYAITFAMRLDRKI 120
TSHR miniTMD DLYTHSEYYNHAIDWQTGPGC WYT-AFAMRLDRKI 37
TMH4 ECL2 TMH5
TSHR TMD RLRHACAIMVGGWVCCFLLALLPLVGISSYAKVSICLPMDTETPLALAYIVFVLTLNIVA 180
TSHR miniTMD RLRHA ALLPLVGISSYAKVSICLPMDTETPGALAYIV 74
TMH5 ICL3 TMH6 ECL3
TSHR TMD FVIVCCCYVKIYITVRNPQYNPGDKDTKIAKRMAVLIFTDFICMAPISFYALSAILNKPL 240
TSHR miniTMD PQYNPGDKDT AILNKPL 91
ECL3 TMH7 ICL4 TMH8
TSHR TMD ITVSNSKILLVLFYPLNSCANPFLYAIFTKAFQRDVFILLSKFGICKRQAQAYRGQRVPP 300
TSHR miniTMD ITVSNSKILLV 102
TSHR TMD KNSTDIQVQKVTHDMRQGLHNMEDVYELIENSHLTPKKQGQISEEYMQTVL 351
TSHR miniTMD 102
C
ECL1
ECL2
ECL3
K660
D619
R519
D
ECL2
C494
ECL3
ECL1
C569

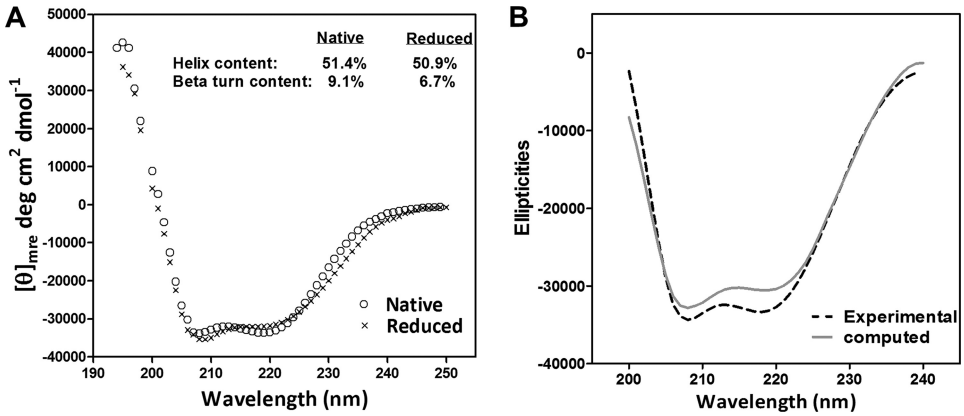

FIGURE 2. **Secondary structure characterization of the mini-TMD protein using far-UV CD spectroscopy.** *A*, representative CD spectra of the purified mini-TMD protein was recorded in the presence (marked by ×) or absence (*open circles*) of the reducing agent and are presented as $[\theta]_{mre}$, mean residue ellipticity. The percentage α-helical and β-sheet contents was calculated as described under "Experimental Procedures." *B*, shown is a comparison of the theoretical (*solid lines*) and the experimental (*dotted line*) CD spectra of mini-TMD protein. The theoretical spectra was computed from the average structure extracted from the molecular dynamic simulation cascade of the modeled mini-TMD protein using the CD analysis tool DichroCalc (31) and plotted against the recorded spectra. Aromatic or side chain-side chain transition parameters were not selected during the computation.

Mini-TMD—The mini-TMD protein, modeled on TSHR TMD, retained these conserved interactions and also maintained the relative positions of the juxtamembrane residues with respect to the membrane (Fig. 1*D*).The stereochemical validations of the mini-TMD revealed G-factor scores to be −0.28, with 93% residues in the allowed region of the Ramachandran plot (data not shown), confirming the robustness of the modeling procedure and a probable reason for its high solubility despite its chimeric nature. The model of the mini-TMD protein displayed an α-carbon r.m.s.d. of 0.3 Å in the helical segments and 1.1 Å for ECLs when compared with TMD, suggesting stabilization of the loop conformation through helical tethers.

The presence of actual α-helical segments in the mini-TMD protein was demonstrated by the far UV CD spectroscopy of the native and the reduced forms of the protein. As shown in Fig. 2*A*, this protein showed 51.4 and 50.9% α-helicity in presence and absence of the reducing agent, respectively, indicating the presence of helical tethers introduced for stabilization of the ECLs. A comparison of the experimentally derived and theoretical CD spectra computed from the MD-simulated structure of the mini-TMD protein using the online CD analysis tool DichroCalc (31) showed a close correlation between the model and the purified protein (Fig. 2*B*), further demonstrating the likelihood of similar secondary characteristics of the mini-TMD protein as predicted. The helical content of the computed spectra was found to be 63% as compared with the experimentally derived helical content of 52%. Interestingly, a decrease in the β-turn content from 10 to 6% due to treatment with reducing agents is intriguing, as the ECL2 of TSHR was shown to possess a β-hairpin-like motif stabilized via a disulfide bridge between Cys-569 (ECL2) and Cys-494 (TMH3) (32). Maintenance of the disulfide bridge in the soluble mini-TMD protein is expected to provide a loop conformation similar to that of the full-length TMD.

Generation of the mini-TMD Antibodies; Specific Interactions with ECLs of Other Members of GpHR Family

The soluble mini-TMD protein was loaded onto Ni^{+2}-NTA-Sepharose column in 20 mM sodium phosphate buffer containing 300 mM NaCl and 5 mM imidazole, pH 7.4, and eluted with increasing concentrations of imidazole (Fig. 3*A*). The purity of the mini-TMD protein eluted with 300 mM imidazole (peak 2) was ascertained by SDS-PAGE and Western blot analysis with an anti-His-tag antibody (Fig. 3*B*). The antibodies raised against the mini-TMD protein could bind to the cognate antigen in ELISA (data not shown) as well as to the full-length TSHR in immunoblot analysis (Fig. 3*C*). Interestingly, the mini-TMD antibodies also recognized FSHR and LHR in immunoblotting (Fig. 3*C*) and flow cytometric analyses (Fig. 4*Ai*) indicating cross-reactivity to two other GpHRs. Binding of the mini-TMD antibodies to LHR and FSHR was found to be 93 and 70%, respectively, that observed with TSHR, which may be attributed to 66 and 60% sequence identity (80 and 72% of sequence similarity) to the mini-TMD protein shares with LHR and FSHR ECLs, respectively (Fig. 4*B*). However, the antibody did not cross-react with HEK293 cells transfected with D2-do-

FIGURE 1. **Modeling and design of GpHR mini-TMD.** *A*, shown are orthogonal views of the alignment of the ECL/ICL-deleted model of TMD and TMH templates used for homology modeling. The *colored helices* denote TMHs derived from the templates used in comparative modeling the TMD (see "Experimental Procedures"), whereas the *gray helices* represent TMHs derived from the model of TSHR TMD. The *numbers in parenthesis* denote the Cα r.m.s.d. values of the given TMH with its corresponding template. *B*, shown is the sequence alignment of TSHR TMD and mini-TMD. *Green*, *blue*, and *yellow arrows* indicate TMH, ECLs, and ICLs, respectively. The mini-TMD residues bearing homology to TMD are shown in *black*, whereas the non-identical residues and gaps are shown in *red*. *C*, shown is molecular modeling of TSHR TMD with the TMHs shown in *green* and the ECLs in *blue*. The highly conserved ionic bridge present in class A G protein-coupled receptors between the Asp/Glu motif in TMH6 (Asn-519 in TSHR) and R3.50 (Ballesteros Weinstein numbering) in TMH3 (Asp-619 in TSHR) as well as the signature GpHR residue (see "Results") Lys-660 in TMH7 are shown in *red*. *D*, shown is the design of mini-TMD protein based on the TSHR TMD model. The *green residues* indicate the helical tethers and synthetic linkers. The ECLs are represented in *blue*, and the computational corrections introduced to maintain the spatio-geometric restraints are shown in *brown*. The probable disulfide bridge between Cys-24 and Cys-59, corresponding to Cys-494 and Cys-569 of TSHR TMD is shown in *yellow*.

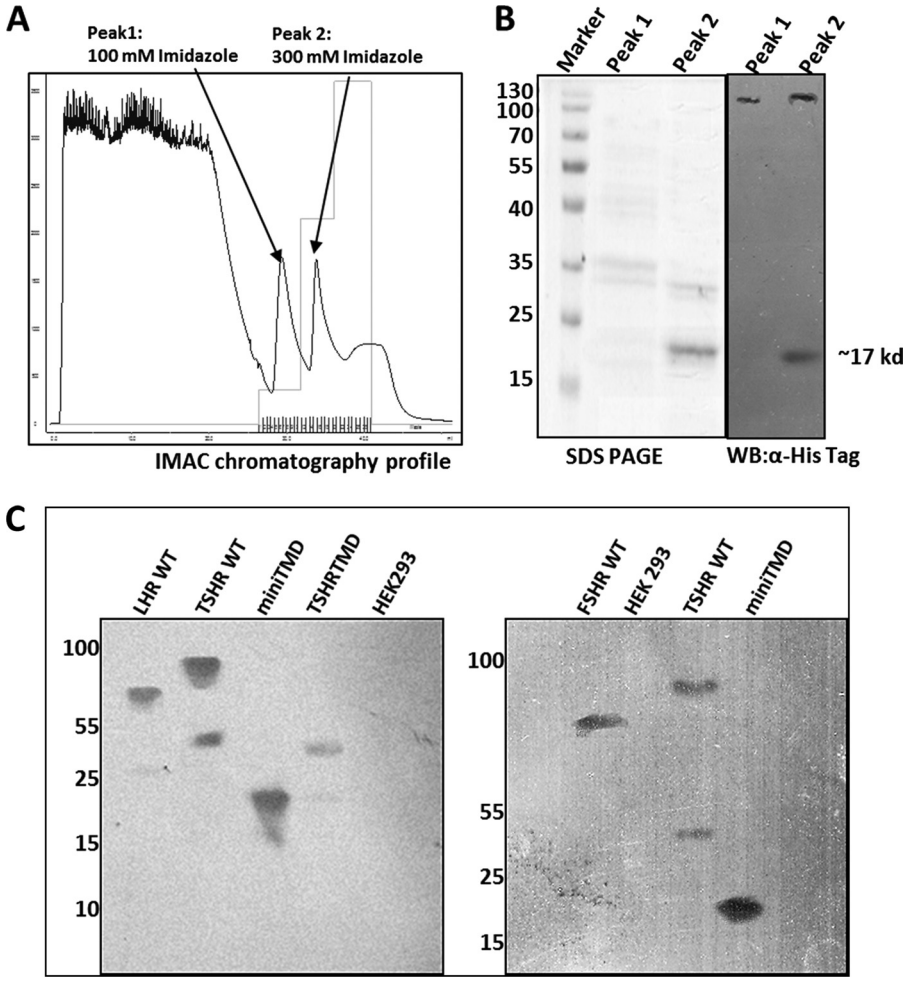

FIGURE 3. *A*, shown is purification of the mini-TMD protein using Ni^{+2}-NTA immobilized metal ion affinity chromatography (*IMAC*). *Peaks 1* and *2* show the proteins eluted with 100 and 300 mM imidazole, respectively. *B*, shown are SDS-PAGE and Western blot (*WB*) analyses of the proteins obtained from peak 1 and 2 of the Ni^{+2}-NTA chromatography using the anti-His-tag monoclonal antibody (GE BioSciences). *C*, specificity of the mini-TMD antibody is shown. The membrane preparations obtained from cell lines expressing TSHR/LHR/FSHR, TSHR TMD, or HEK293 cells were solubilized with 1.2% digitonin and electrophoresed on 10% (*left panel*) or 7.5% (*right*) SDS, transferred to PVDF membrane, and probed with the mini-TMD antibodies. TSHR ECL protein was used as a positive control.

pamine receptor or M4-muscarinic receptor (data not shown), clearly indicating the specificity of the mini-TMD antibodies.

Effect of the Mini-TMD Antibodies on Hormone Action

The mini-TMD antibodies exhibited different effects on hormone binding and response. The antibodies had no effect on binding of ^{125}I-labeled human FSH/TSH to the respective receptors when they were added before the addition of the hormone, whereas a marginal decrease was observed in the case of hCG binding to LH receptor (Fig. 5*A*). In contrast, preincubation of cells with the antibodies inhibited hormone response in a dose-dependent manner in the case of all three receptors (Fig. 5*B*). Furthermore, the dose-response curves for the hormones (human TSH and hCG) exhibited a decrease in R_{max} without any changes in EC_{50} in the presence of the mini-TMD antibodies, clearly indicating that the antibodies exhibit non-competitive antagonism (Fig. 5, *C* and *D*).

Effect of Hormone Binding on Receptor-Antibody Interactions

The non-competitive antagonism exhibited by the mini-TMD antibodies indicated that the antibodies either inhibit ECLs/TMH from attaining a conformation required for hormonal activation or they interfere in the critical secondary contacts between the hormone and ECD and/or ECLs. Although the first possibility may be ruled out by the oligoclonal nature of the antibody, precluding specificity to any given loop conformation, the second possibility will result in loss of access of the ECLs to the antibodies in the preformed hormone-receptor complex. Hence, the cells expressing TSHR/LHR/FSHR were first incubated with or without the respective hormones (10 nM) at 4 °C followed by incubation with the saturating concentrations of the mini-TMD antibodies (20 μg/ml) and determination of antibody binding by flow cytometry. As shown in Fig. 4*Aii*, preincubation with the hormones significantly decreased the subsequent antibody binding to all three receptors, indicating loss of epitopes (ECLs) post-hormone binding.

Effect of the Mini-TMD Antibodies on Mutant GpHR Receptors; Differential Interactions of GpHR HinRs with Their ECLs

The above experiment as well as the previously proposed contact between hormone α-L1 and L3 loops and the ECLs (33) emphasize the critical role played by the loops in mediating the

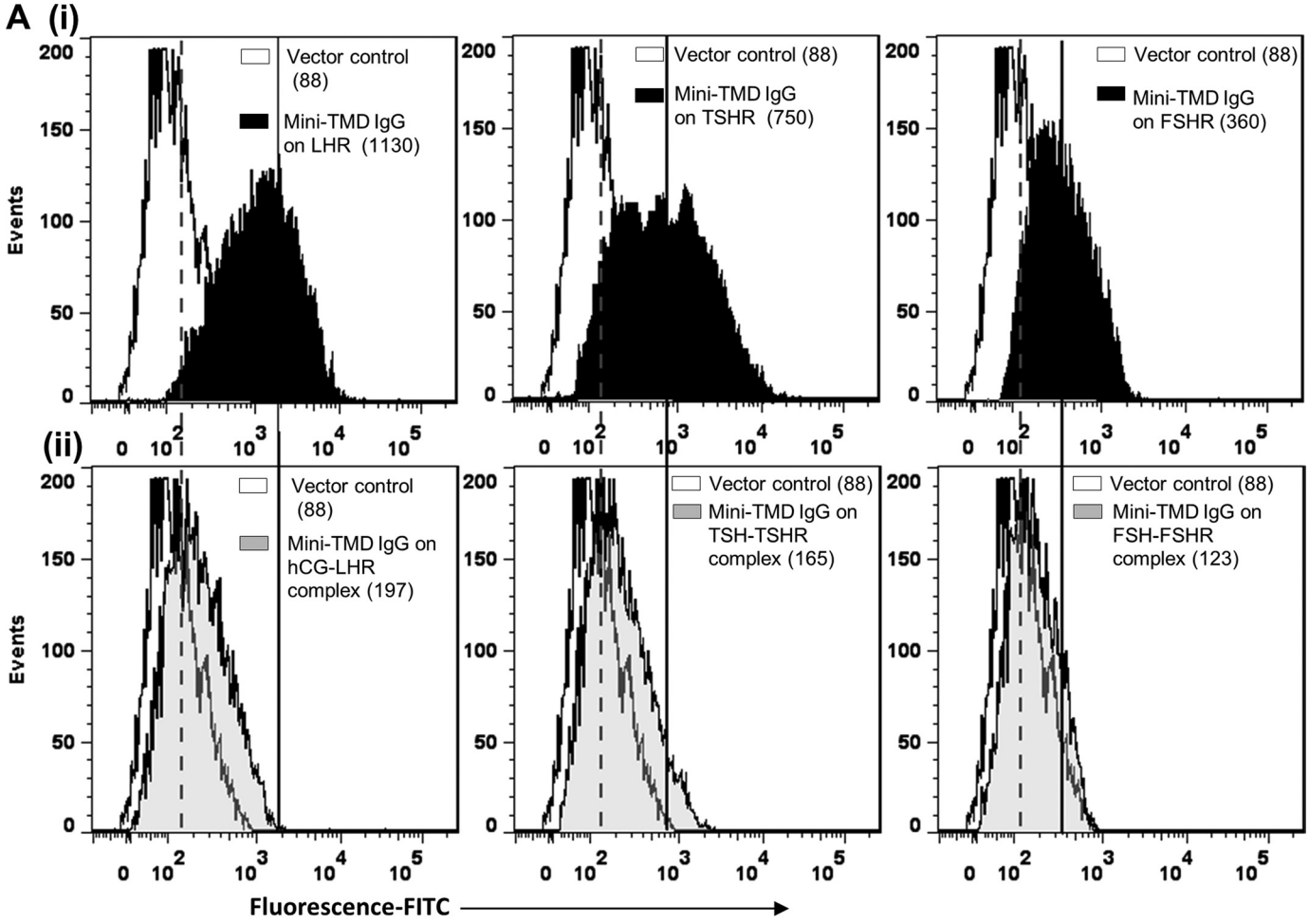

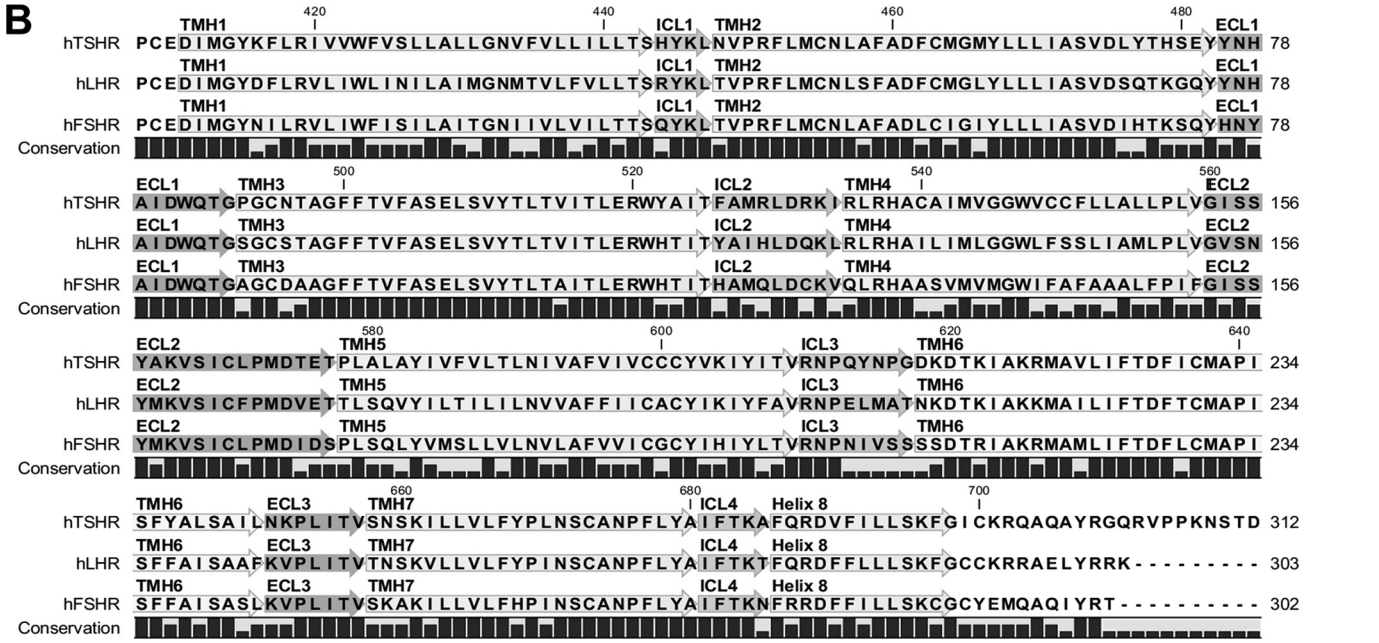

FIGURE 4. **Binding of the mini-TMD antibodies to receptor and hormone-receptor complex.** *Ai*, shown is a flow cytometric analysis of binding of the mini-TMD antibodies (20 μg/ml) to HEK293 cells expressing LHR (*left panel*), TSHR (*middle panel,*) or FSHR (*right panel*). *Aii*, HEK293 cells expressing the LHR (*left panel*), TSHR (*middle panel*), or FSHR (*right panel*) were previously saturated with their respective hormones (10 nM), and binding of the mini TMD antibodies (20 μg/ml) was monitored by flow cytometry (*gray histograms*). In both Fig. *Ai* and *Aii*, the *white histograms* indicate binding of the mini-TMD antibodies to the mock-transfected HEK293 cells. The *broken* and *unbroken lines* designate the median fluorescence intensity of the *gray histograms* and *black histograms*, respectively, measured in the same experiment. *B*, multiple sequence alignment of the transmembrane domains of the three glycoprotein hormone receptors is shown.

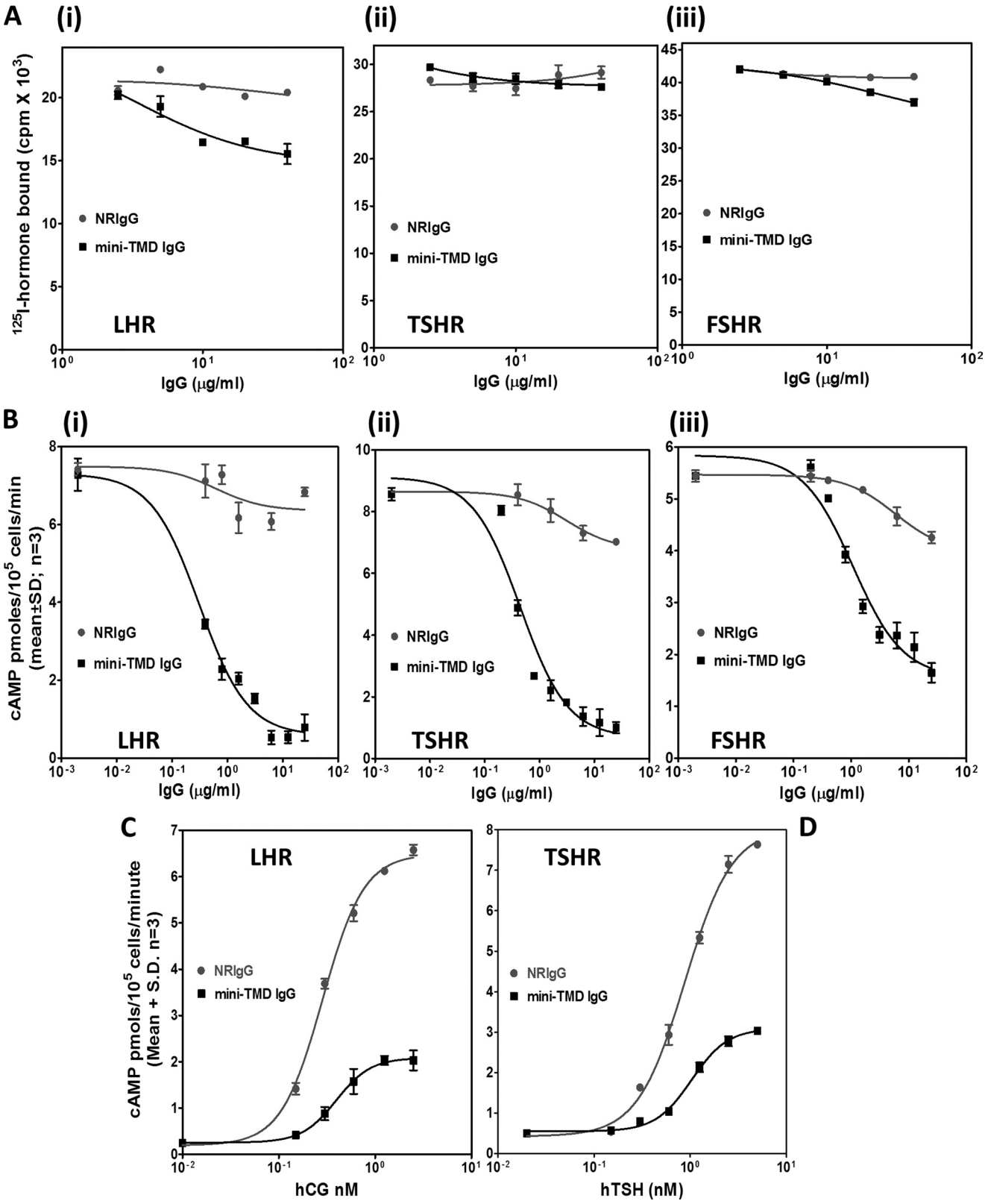

FIGURE 5. **Effect mini-TMD antibodies on hormone-receptor interactions.** *A*, increasing concentrations of the mini-TMD antibodies were preincubated with HEK293- TSHR/LHR/FSHR membrane preparations (5 μg) at 37 °C followed by the addition of respective radioiodinated hormones, and the receptor bound hormone was determined: hCG-LHR (*Ai*), TSH-TSHR (*Aii*), and human FSH-FSHR (*Aiii*). *B*, the effect of the mini-TMD antibodies on hormone-stimulated response was determined by preincubating the cells expressing the individual receptors with increasing concentrations of the mini-TMD antibodies or NRIgG for 1 h at 37 °C followed by incubation with 5 nM concentrations of the respective hormones for 15 min at 37 °C and determining cAMP produced by RIA: LHR (*Bi*), TSHR (*Bii*), FSHR (*Biii*). *C* and *D*, the cells expressing LHR (*C*) and TSHR (*D*) were incubated with the mini-TMD antibodies (1 μg/ml) for 1 h followed by the addition of increasing concentrations of the respective hormone for 15 min, and cAMP produced was determined by RIA.

hormone-stimulated response. The role of ECLs in maintenance of the basal or ligand-independent receptor activation is not clearly understood. The contribution of the HinR in maintaining the basal cAMP production in GpHRs is particularly important through the selective interactions with the critical residues in the ECLs (34). To provide a physical basis for the HinR-ECL interactions, the effects of the mini-TMD antibodies on cAMP production by the HinR point and truncation mutants were investigated, and accessibility of their ECLs to the mini-TMD antibodies was monitored by flow cytometry.

Binding of the Mini-TMD Antibodies to GpHR-truncated Mutants—WT (*SP*) and LRR-deleted (*HinR*) or ECD-deleted (*TMD*) mutants of all three GpHRs (schematically shown in Fig. 6*A*) were transfected in HEK293 cells, and binding of the mini-TMD antibodies or respective hinge-specific antibodies was monitored by flow cytometry (Fig. 6*B*). The ratio of RMFIs for the mutant and WT receptors ($RMFI_{MUT}/RMFI_{WT}$) using the HinR antibodies was indicative of the relative cell surface expression of the mutant receptors (R*e*), whereas the ratio of RMFIs for WT and mutated receptors using the mini-TMD antibodies indicated the relative accessibility of ECLs in the mutant receptors (R*a*).

As seen in Fig. 7*A*, although R*e* values of TSHR and FSHR HinTMD mutants were comparable (69 and 71% of WT expression, respectively), expression of LHR HinTMD was 40% that of LHR WT expression. Accessibility of ECLs of TSHR/FSHR HinTMD to the antibodies was proportionate to their cell surface expression, suggesting binding of antibodies was similar in WT and LRR-deleted mutants of TSHR/FSHR, and hence, the relative orientation of the hinge with respect to ECLs did not differ substantially in the LRR-deleted and WT receptors. On the other hand, the relative accessibility of LHR HinTMD to the mini-TMD antibodies was considerably higher. This relatively higher binding of the mini-TMD antibodies to LHR HinTMD as compared with FSHR or TSHR HinTMD suggests that LHR hinge has a more open conformation with respect to the ECLs and has a lesser constraint on the ECLs.

More interestingly, binding of the mini-TMD antibodies was highest to LHR TMD followed by FSHR and TSHR TMDs, indicating that although considerable sequence identity exists among the ECLs of the three receptors, their relative conformations are different, pointing out to a very important role of TMH in maintaining ECL conformations. However, R*e* values for the ECD deleted mutants were not available in the absence of appropriate normalizing antibodies such as the HinR antibodies used for LRR-deleted mutants.

Effect of the Mini-TMD Antibodies on the Basal cAMP Levels of the Receptor-truncated Mutants—As seen in Fig. 7*B*, the WT basal activities of GpHRs in terms of hormone-independent cAMP production vary widely, with TSHR being the "noisiest" receptor followed by FSHR and LHR. Moreover, as reported previously, removal of ECD further increased cAMP production for both TSHR and FSHR (7, 35). This high basal cAMP level in TSHR/FSHR TMD mutants decreased by the introduction of HinR in the HinTMD mutants, suggesting that HinRs act as a tethered inverse agonist to the TMD, direct evidence for their roles in maintaining the basal as well as hormone-independent receptor activation (7, 24).

Interestingly, the higher basal cAMP production did not occur on removal of LHR ECD, indicating a lack of built-in inverse agonism of LHR ECD. Similar observations regarding the intrinsic low basal cAMP production of LHR have also been made with LHR-truncated mutants expressed as a HA-tag vasopressin receptor fusion protein (36).

The high basal cAMP production activities of TSHR WT and TSHR/FSHR TMD mutants decreased in the presence of the mini-TMD antibodies. The effect of antibodies was significantly more in the case of the TMD mutants compared with WT, indicating that HinR probably modifies the accessibility of ECL to antibodies. However, the antibodies had a marginal effect on the basal activities of LHR or FSHR WT.

Effect of the Mini-TMD Antibodies on HinR and ECL Activating and Inactivating Mutations—Several residues in HinR of GpHRs have been implicated in maintenance of the basal cAMP levels of which the serine in the highly conserved YPSHCCAF motif seems to be most critical. Mutations in this residue (TSHR, Ser-281; LHR, Ser-277; FSHR, Ser-273) lead to constitutive activation of the receptor as a result of a conformational shift from a "closed" constrained receptor state to an "open" unconstrained receptor (37). The accessibility of ECLs in such mutants to the mini-TMD antibodies would provide a clear picture on the spatial orientation of the HinR with respect to the ECLs during the activation process. TSHR and LHR serine mutants (TSHR, S281I; LHR, S277Q) displayed R*e* values of 0.48 and 0.42, respectively (48 and 42% of WT expression) computed using the respective HinR antisera as control antibodies, clearly suggesting reasonable surface expression (Fig. 8, *Ai* and *Bi*). Interestingly, as shown in Fig. 8, *Aii* and *Bii*, the mini-TMD antibodies showed higher binding to both TSHR (S281I) and LHR (S277Q) mutants as compared with the WT receptor (*Ra* values of 1.6 and 0.85, respectively), indicating higher accessibility of the ECLs in these mutants. Intriguingly, binding of the antibodies to the mutant receptor with inactivating mutation D410N at the C-terminal end of the TSHR ECD was found to be considerably higher than either the WT or the HinR activating mutations ($Ra = 2.12$, surface expression = 63% that of WT expression ($Re = 0.63$)).

We also created three activating mutations residing in each of the ECLs of TSHR (ECL1, I486F; ECL2, I586T; ECL3, V656F), and binding of the mini-TMD antibodies was investigated. All three mutants displayed 65–75% relative surface expression compared with the WT receptor. However, binding of the mini-TMD antibodies (and hence the relative accessibilities) varied among the three mutants with I486F ($Ra/Re = 3.4$) showing the highest binding followed by V656F ($Ra/Re = 1.7$) and finally, I568T ($Ra/Re = 1.6$) (Fig. 9*Ai*).

More interestingly, the high basal cAMP production of both HinR as well as ECL activating mutations was dampened in the presence of the mini-TMD antibodies (Figs. 8, *C* and *D*, and 9*Aii*). In addition, the hormone-stimulated response of the serine mutants of LHR and TSHR was also inhibited in the presence of the mini-TMD antibodies, although the degree of inhibition of "expression-normalized" response in the case of the mutant receptor was lower (46% for LHR, 37% for TSHR) than those of the WT receptors, which was 68 and 72% for TSHR and LHR, respectively (Fig. 8, *C* and *D*). Inhibition of the hormone-

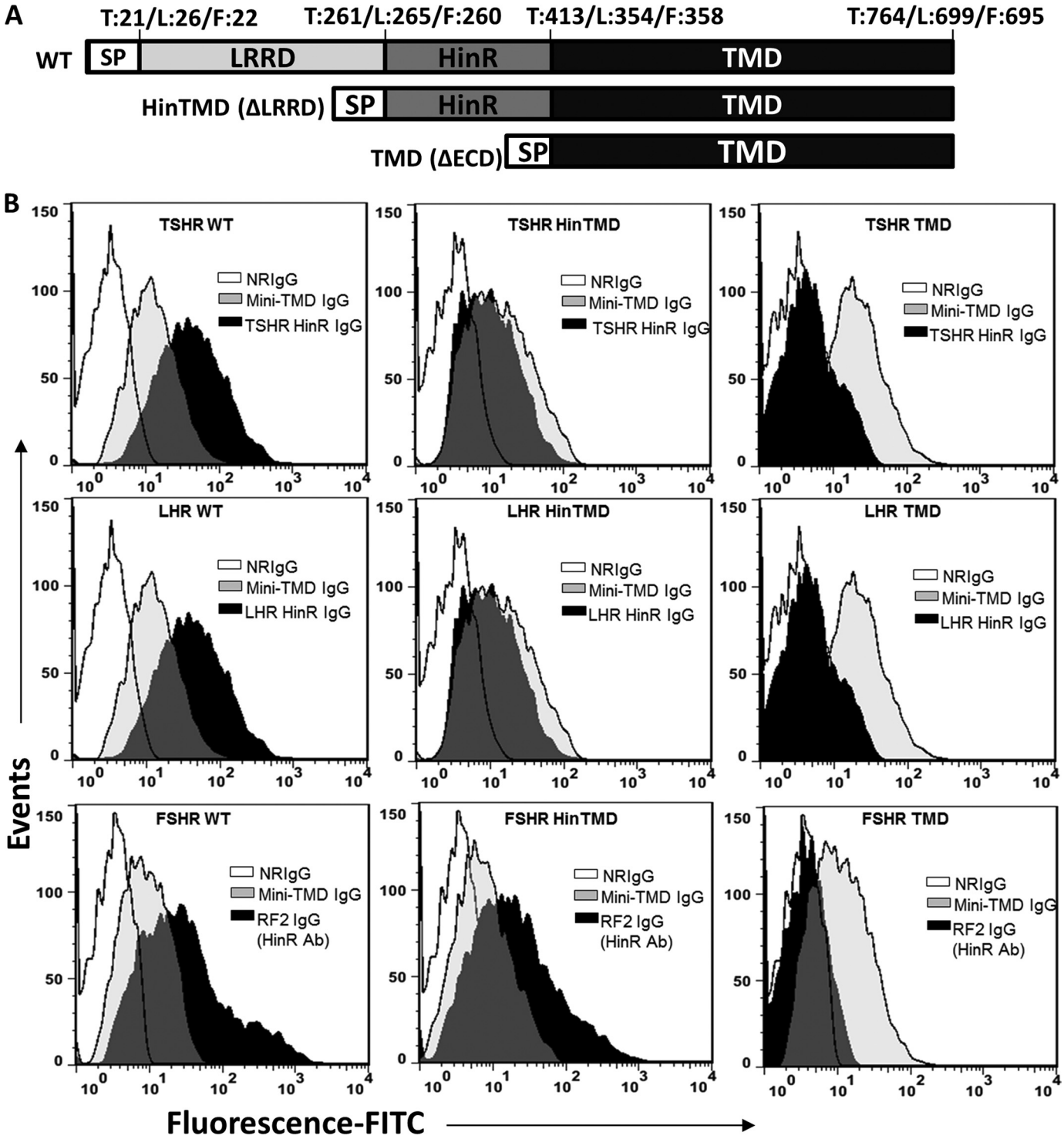

FIGURE 6. **Relative binding of the mini-TMD antibodies to GpHR deletion mutants.** *A*, schematic representation of GpHR deletion mutants is shown. The putative residues marking the start of a given domain are mentioned for each receptor; *T*, TSHR; *L*, LHR; *F*, FSHR; *SP*, signal peptide. *B*, HEK293 cells transiently transfected with the full-length WT receptor or HinTMD and TMD deletion mutants were incubated with either NRIgG (*open histograms*) or 1 μg/ml concentrations of the mini-TMD antibodies (*gray histograms*), and antibody binding was determined by flow cytometry. The surface expression of each mutant was ascertained using the respective HinR-specific antibodies (10 μg/ml) shown as *black histogram*.

stimulated response of the ECL mutants was not carried out due to the poor stimulation of these receptors making analysis unreliable.

Effect of the Mini-TMD Antibodies on TSHR-LHR Chimeric Receptors—The higher accessibility of ECLs to mini-TMD antibodies in LHR HinTMD as compared with TSHR HinTMD suggests that the interactions of the LHR HinR with its ECLs were less stringent as compared with those of TSHR. Binding of mini-TMD antibodies to the chimeric receptor where the HinR of TSHR has been replaced by LHR (TSH-LHR-6) was investigated. Expression of this mutant on the cell surface, as demonstrated by binding of the TSHR-LRR-specific antibodies (Fig.

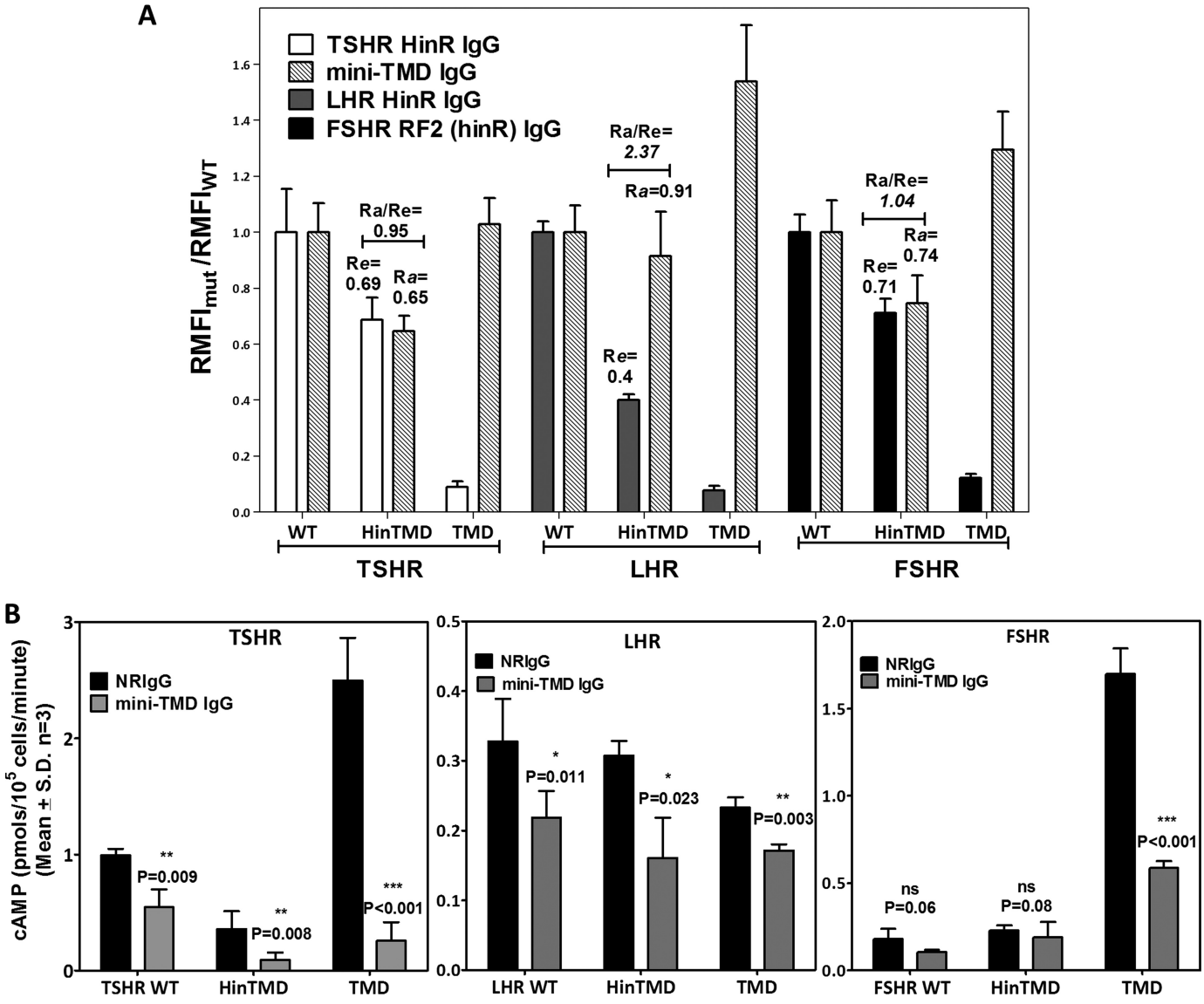

FIGURE 7. **Effect of the mini-TMD antibodies on GpHR deletion mutants.** *A*, the ratio of RMFI for the mutant/WT was determined using the respective HinR-specific antibodies to estimate the relative expression of the mutant on cell surface and is designated as R*e* (24). Similar ratios were determined for the mini-TMD antibodies to determine the relative accessibility of the epitope in mutants and designated as R*a*. An R*a*/R*e* >1.2 indicates higher binding of the mini-TMD antibodies to the mutant as compared with the WT. Each *bar* represents RMFI ratios of three experimental replicates repeated three times. *B*, the WT and deletion mutants (HinTMD and TMD) of all the three GpHRs were transiently transfected, their basal cAMP production was measured in the presence of NRIgG or the mini-TMD antibodies (10 μg/ml) after 1 h of incubation, and cAMP produced was normalized to their cell surface expression (as determined in *A*). The statistical significance was compared with the respective pre-immune IgG control and is denoted by the *p* value calculated from the two-tailed unpaired *t* test.

10*Ai*) was marginally lower than the WT receptor (86%, R*e* = 0.86). Interestingly, binding of the mini-TMD antibodies to the chimeric receptor (Fig. 10*Aii*) was found to be higher (200%) than to the TSHR WT receptor, suggesting the presence of LHR HinR influences the accessibility of the ECLs to these antibodies (Fig. 10*Aiii*). As in the case of LHR, the mutant exhibited much lower basal cAMP production rate than TSHR WT. Response of the chimeric receptor to TSH was also inhibited in the presence of the mini-TMD antibodies, suggesting LRR independent action of these antibodies (Fig. 10*B*).

Effect of the Mini-TMD Antibodies on LHR TMH Activating Mutations; Clues to the Mechanism of Inhibition of Mini-TMD Antibodies—Effect of mini-TMD antibodies on the constitutively active mutants of LH receptor caused by mutations in TMH leading to precocious puberty was next investigated. Expression of activating mutants L457R present in TMH3 and D578Y present in TMH6 on the cell surface was confirmed by flow cytometry with LHR hinge antibodies. As seen in Fig. 9*B*, the mutants exhibited high basal cAMP production and poor response to hCG. The mini-TMD antibodies were able to decrease the constitutive activities of both mutant receptors, inhibition of D578Y (Fig. 9*Bi*) being much greater than that of L457R (Fig. 9*Bii*).

DISCUSSION

Importance of the extracellular loops of GpHR in signal transduction is evident from several somatic and germ line mutations that cause abnormal receptor function (38). How-

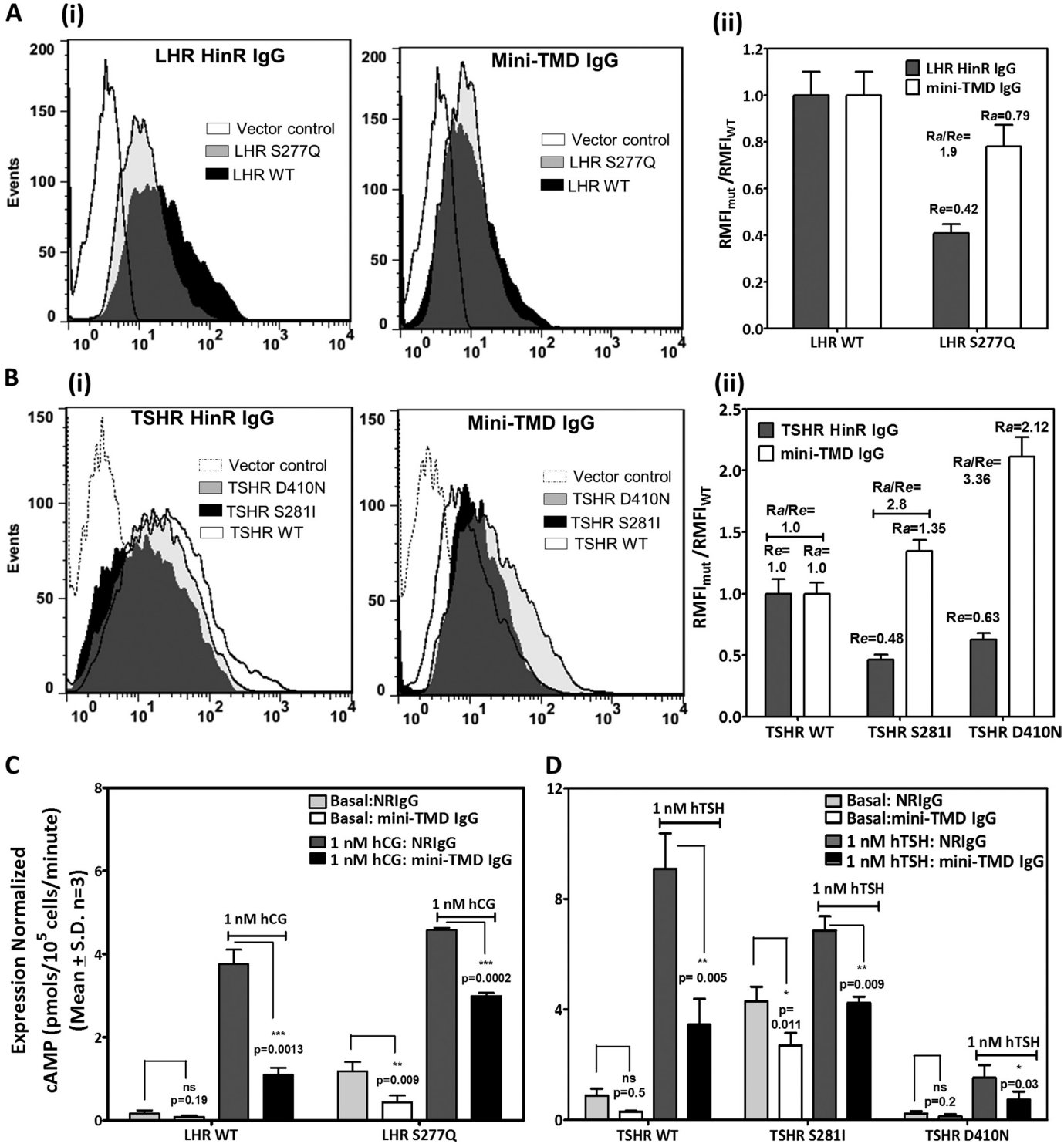

FIGURE 8. **Effect of the mini-TMD antibodies on the HinR activating and inactivating mutations of TSHR and LHR.** *A* and *B*, flow cytometric analysis of HEK293 cells transfected with the WT or different HinR mutants of LHR (*panel A*) or TSHR (*panel B*) using the HinR-specific antibodies (10 μg/ml) and the mini-TMD antibodies (1 μg/ml) is shown. Accessibility of epitopes to the mini-TMD antibodies to the HinR mutants was estimated by R*a* of the mutants with respect to the WT LHR (*Aii*) or TSHR (*Bii*) as mentioned in the legend of Fig. 7*A*. *C* and *D*, the hormone-stimulated and the basal cAMP production of LHR CAM S277Q (*C*) and TSHR HinR mutants S281I and D410N (*D*) was measured in the presence of NRIgG or the mini-TMD antibodies (10 μg/ml). *hTSH*, human TSH.

ever, the precise mechanism of the signal transduction has not been elucidated. In this study the antibodies recognizing GpHR ECLs in their native forms have been used to understand the signaling mechanism of GpHRs. The antibodies raised against TSHR-TMD inhibited the basal and hormone-stimulated cAMP production by all three GpHR without affecting the hormone binding. The antibodies also suppressed the high basal activities of gain-of-function mutations in the HinRs, exoloops, and TMDs such as those involved in precocious puberty and thyroid toxic adenomas. Thus, these antibodies, whereas pro-

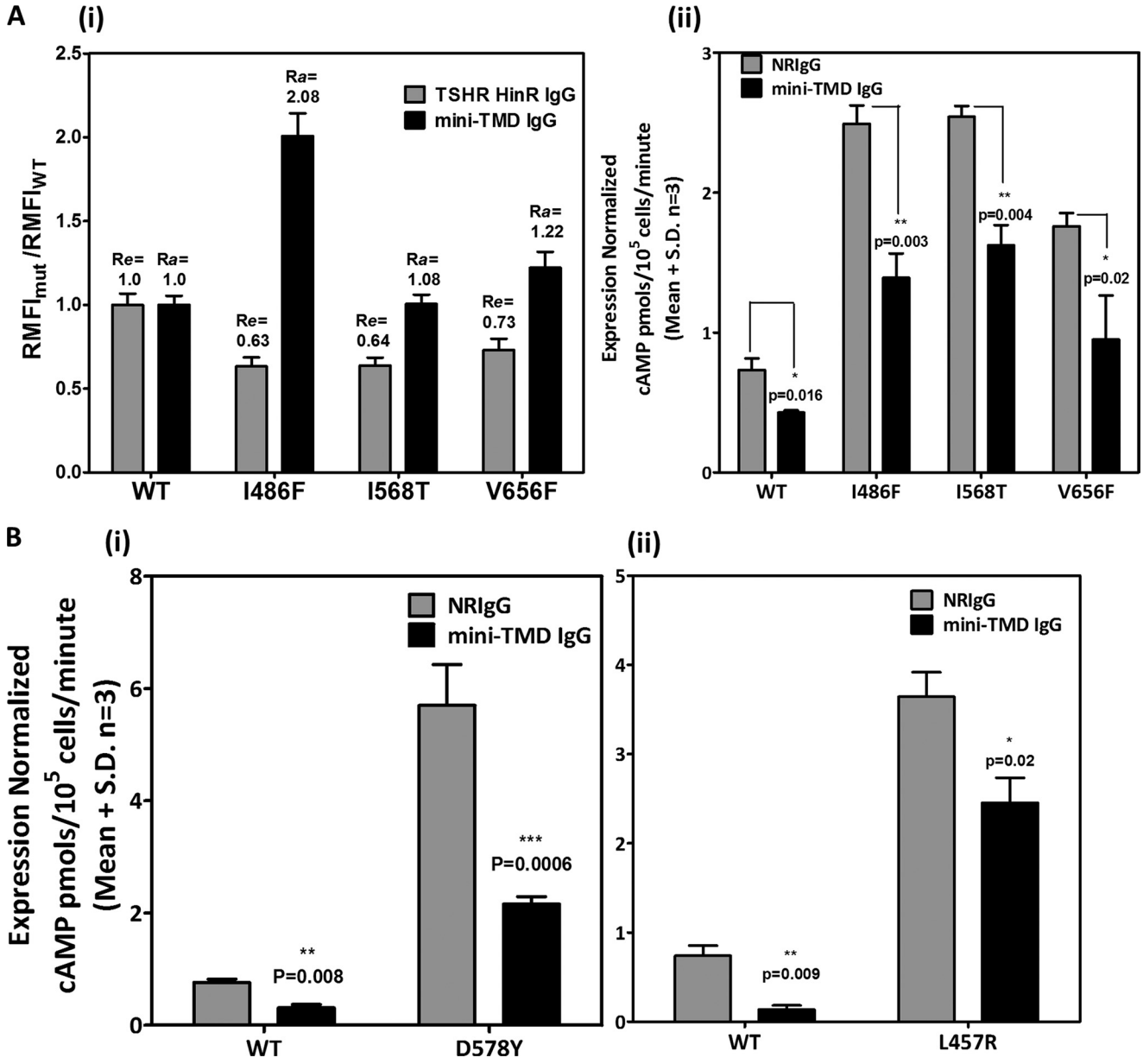

FIGURE 9. **Effect of the mini-TMD antibodies on the activating mutations of TSHR ECLs and LHR TMD.** Flow cytometric analysis of HEK293 cells transfected with the WT or TSHR ECL CAMs (*Ai*) using the mini-TMD antibodies (1 μg/ml) and the RMFI values so obtained were normalized to those using the HinR-specific antibodies. Basal cAMP production of TSHR ECL CAM (*Aii*), LHR TMD CAM D578Y (*Bi*), and L457R (*Bii*) was estimated in the presence of 10 μg/ml of preimmune IgG (*gray bars*) or mini-TMD IgG (*black bars*).

viding interesting insights into receptor activation, also provide interesting therapeutic strategy for treating conditions such as precocious puberty and thyroid adenomas.

The method of designing a mini-TMD protein used as an antigen not only overcame issues such as solubility and poor expression but allowed retention of a degree of the native conformation of the TMD as demonstrated by the near native helical content in the CD spectra of the protein. More importantly, retention of the β turn motif in the ECL2 and disulfide bridge between ECL2 and TMH3 ensured generation of conformation-specific antibodies against the protein. The main goal of this study was to provide answers to the following pertinent questions; (*a*) the spatial organization of the loops in the absence and presence of the hormone, (*b*) the interaction (or lack thereof) of the HinR with the ECLs, (*c*) a comparative analysis of ECLs of the three GpHRs during hormone-dependent and -independent activation, and (*d*) a holistic view of ECLs as a functional receptor unit and not just determination of a few critical residues involved in the signal transduction process.

Spatial Organization of the Loops in the Resting and Hormone-stimulated Receptor; Hormonal Contact with ECLs Causes the ECLs to Become Buried Inside the TMH—The interactions between the α-subunit and ECLs or hinge-ECL after the initial hormone binding to LRRs are probably the critical events in hormonal activation of the receptors. Preferential photo-affinity labeling of the α subunit of hCG by the HinR and exoloop 2 peptide (33), inhibition of hormone response by the α-subunit specific antibodies without any effect on hormone binding (40),

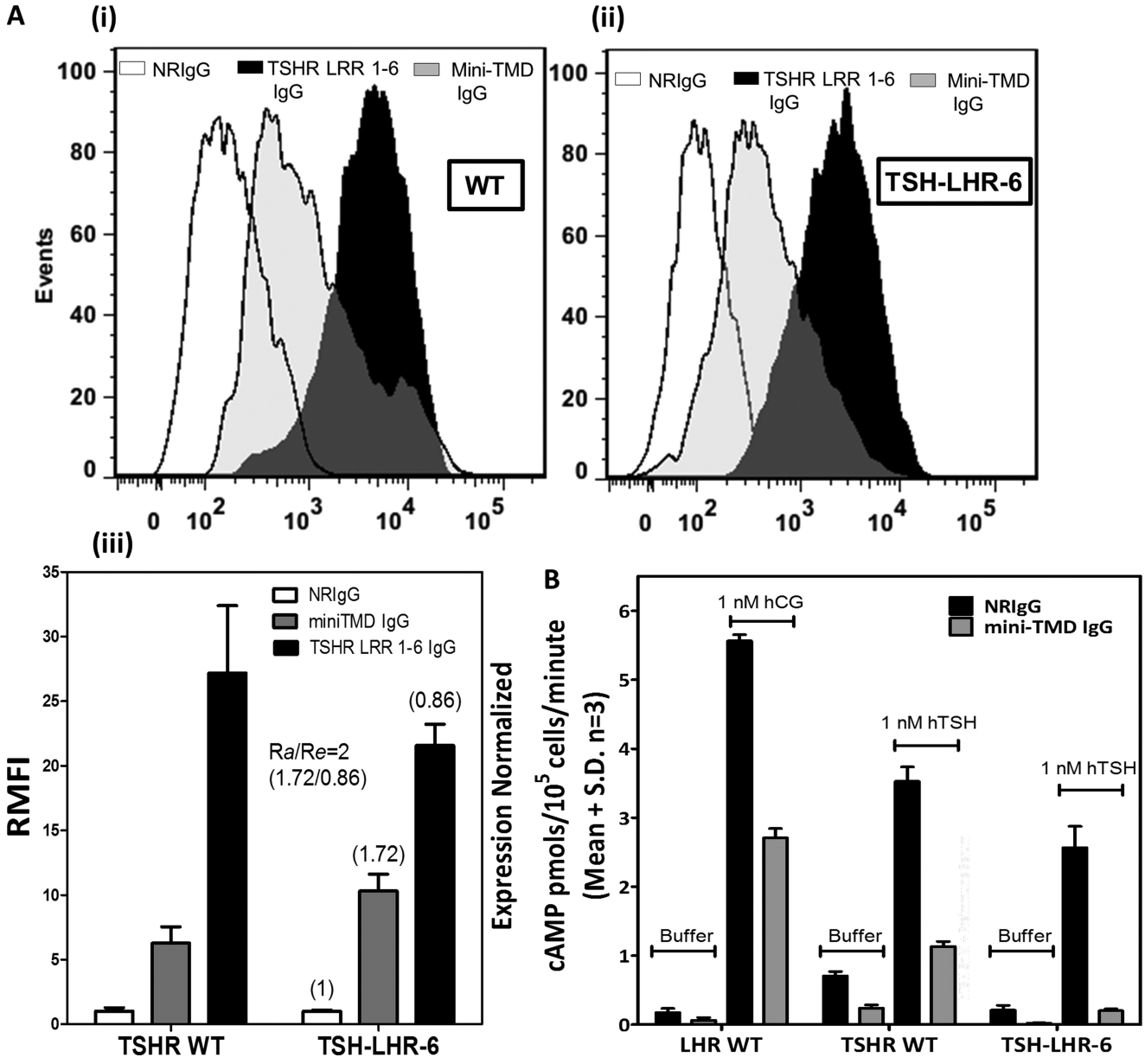

FIGURE 10. **Effect of the mini-TMD antibodies on TSHR-LHR chimeric mutant.** *A*, binding of antibodies to TSHR WT (*Ai*) and HinR chimeric mutant TSH-LHR-6 (*Aii*) was monitored by flow cytometry using the TSHR LRR 1–6 specific IgG (*black bars*) and the mini-TMD antibodies (*gray bars*). The mean fluorescence intensities of each antibody for the WT and TSH-LHR-6 receptor, as derived in Fig. *Ai* and *Aii*, were normalized to preimmune IgG (*NRIgG*, *white bars*) and expressed as RMFI (*Aiii*). *Numbers in parentheses over each bar* represent the ratio of RMFI of TSH-LHR-6 of a given antibody to those obtained with the WT receptor. *B*, hormone-stimulated and basal cAMP production of LHR WT, TSHR WT, and TSH-LHR-6 was measured in the presence of NRIgG or the mini-TMD antibodies (10 μg/ml). *hTSH*, human TSH.

and loss of bioactivity in the mutants of the hormones with mutations in the α-subunit (41) indicate such a possibility. The ability of the mini-TMD antibodies to inhibit hormone-stimulated response in all the three receptors without affecting the respective hormone binding strongly supports this hypothesis and also indicates a common mechanism of GpHR activation. Activation of the receptor may occur through the contact of the L1 and L3 loops of the α-subunit with the residues in the hydrophobic core of the juxtamembrane domain after displacement of the second or third extracellular loop (2), or the α-subunit may disengage the HinR from ECL2, leading to TMH relaxation and receptor activation (34). Both conditions may lead to removal of the loops from their hydrophobic environment and should result in higher exposure and, hence, better accessibility of these epitopes to the mini-TMD antibodies. On the contrary, the hormone-bound receptors showed lower binding to the antibodies. This cannot be attributed to internalization of the receptor as the flow cytometry experiments were performed on ice. Moreover, no decrease in binding of the control antibodies to other regions (LRR 1–3 specific antibodies) was observed. These data suggest that the exoloops are buried deep inside the hormone-receptor complex, and the tips of the α subunit may be in contact with ECLs while making additional contact with the TMH residues. This could also possibly explain the contact between ECL and TMH residues and how the double mutant I568V/I640L (ECL2/TMH6) suppresses the increased basal

activity exhibited by I568V alone (32). The lack of inhibition of hormone binding by the antibodies also seems to be contrary to the isolated reports of the ECLs being part of the primary hormone binding site (43, 44), although the evidence from mutational studies of ECL residues suggested a compromise in signaling but not in hormone binding (45, 46).

The HinR-ECL Interaction as the Basis of Basal cAMP Production; Weaker Interactions of Hinge-ECL in LHR as Compared with TSH/FSH Receptors—The low basal cAMP production of LHR or FSHR as compared with TSH (Fig. 8, *C* and *D*) is a hallmark of the physiological regulation by these receptors (47). Even with the remarkable similarity in the receptor architecture, the mechanistic basis of such differential basal receptor activation has been not well elucidated. Removal of the ECD from TSHR further increased the relatively high basal cAMP production, similar to that reported earlier (48). This increase has been attributed to the tethered inverse agonistic effect of the TSHR ECD where the ECD keeps the TMD in an inactive state (49), and this inverse agonism has been narrowed down to the HinR of TSHR where specific contacts between the residues of HinR and ECLs are primarily responsible for the hinge-TMD constraint (50). Supporting this is our observation that high basal cAMP production of TSHR TMD is dampened by the HinR in the TSHR HinTMD mutants (Fig. 8, *C* and *D*). In an earlier study on FSHR (7), we found that deletions in the segment of amino acids 290–331 in the HinR resulted in an increase in the basal cAMP production. These data suggest a common role for the HinR in regulating FSHR and TSHR activities. On the other hand, neither the WT LHR- nor ECD-deleted mutants show a high degree of basal cAMP production, possibly due to different interactions of the LHR HinR with its ECLs (36). This possibility was investigated by determining the relative accessibilities of the TMDs and HinTMDs of all three receptors to the antibodies. LHR HinTMD showed a relative higher antibody binding, suggesting that the HinR of LHR interacts comparatively weakly with its ECLs as compared with those of TSHR or FSHR, and hence, LHR TMD was more accessible to antibodies than its counterparts in TSHR or FSHR. Moreover, even with a higher degree of binding, LHR TMD mutants were relatively less affected by the mini-TMD antibodies as compared with the significant inhibition of TSHR and FSHR TMDs in terms of basal cAMP production, indicating that ECLs of LHR acted in a manner unlike the other two members of GpHR family. A further evidence for a differential involvement of the HinR of LHR is provided with the chimeric TSHR-LHR-6 mutant that responds to TSH but does not exhibit high basal activity of TSHR. The relatively higher binding of the mini-TMD antibodies to TSH-LHR-6 as compared with the TSHR WT also suggests the presence of LHR HinR not only decreases the interaction of HinR with the ECLs but also directly correlates with the basal activation of the receptor.

Both Activating and Inactivating Mutations in GpHRs Cause the HinR to Become Disengaged from ECLs—Transient changes in HinR-ECL interactions in response to the hormone are thought to be mediated by the highly conserved motifs in Cb-2 and Cb-3, especially through the conserved serine in the YPSH-CCAF motif, as mutations at this serine for all the three receptors cause constitutive activation of the receptor (51). This has been attributed to the loss of packing in the aromatic environment at the ECL-TMH interface (52), and it may be hypothesized that the serine mutants in this region undergo a spatial reorganization with respect to ECLs. Both TSHR-Ser-281 and LHR-Ser-277 mutants are characterized by higher binding of the mini-TMD antibodies as compared with the WT counterpart, suggesting that these mutant receptors are less constrained than WT. More interestingly, binding of the mini-TMD antibodies to ECL mutants varied for each loop, with I486F (ECL1) displaying the highest degree of binding followed by V656F (ECL3) and then by I586T (ECL2). The molecular modeling and mutagenesis studies have shown the β-turn of ECL2 to lie on the plane of the TMD interface and would, hence, be expected to have lower accessibility to the mini-TMD antibodies. On the other hand, Ile-486 in ECL1 has been known to form the hydrophobic core of ECLs and interact directly with Ser-281 (52). Hence, one would expect a similar increase in antibody binding to I486F mutant as observed with Ser-281.

In contrast to the discussion above that disengagement of the HinR from the ECL is a necessary and sufficient event for increase in basal cAMP, we find that the mini-TMD antibodies display an even higher binding to the inactivating mutation D410N as compared with Ser-281 or WT receptors. This mutation is characterized by extremely low cAMP basal levels but is capable of stimulation by TSH. Location of D410N is said to be in proximity with ECL3 and ECL1 (30), and mutations in both these ECLs are characterized by higher binding to the mini-TMD antibodies. This would suggest that the hinge-ECL interactions are maintained through equilibrium of pro-active and pro-inactive conformational states, and the active or inactive state of the receptor is a function of position of the perturbation of interaction between these two domains. Simple disengagement of hinge may no longer be considered the only event responsible for maintenance of basal receptor activation.

The Mechanism of Action of Mini-TMD Antibodies; an Experimental and Theoretical Consideration into the Inhibitory Effect of the Mini-TMD Antibodies—As shown here, the mini-TMD antibodies could decrease the basal cAMP production by both WT receptor and activating mutations and inhibit the hormone-stimulated responses of all the three GpHRs. The pan-receptor effects of the mini-TMD antibodies cannot be explained simply by invoking their effects in altering the HinR-ECL interaction, as the constitutively activating mutation in the ECD cannot bypass disruption of signal transduction in the serpentine domain (8). This would indicate that the mini-TMD antibodies must affect critical interhelical interaction as well. The ability of these antibodies to inhibit the high basal activity of the LHR-activating mutations L457R (TMH 3) and D578Y (TMH 6) indicates this possibility. Previous reports suggest that Leu-457 and Asp-578 lie in close proximity, and introduction of a positively charged amino acid at the position 457 generates an attractive effect on Asp-578, thus inducing perturbations in TMH3-TMH6/7 interaction patterns (42). Whether the mini-TMD antibodies influence such helix arrangement through their interactions with the ECLs was investigated by comparing the deviation of the mean structure after MD of the WT and mutant receptors. For this purpose, LHR TMD was modeled using the method adopted for TSHR TMD, the L457R

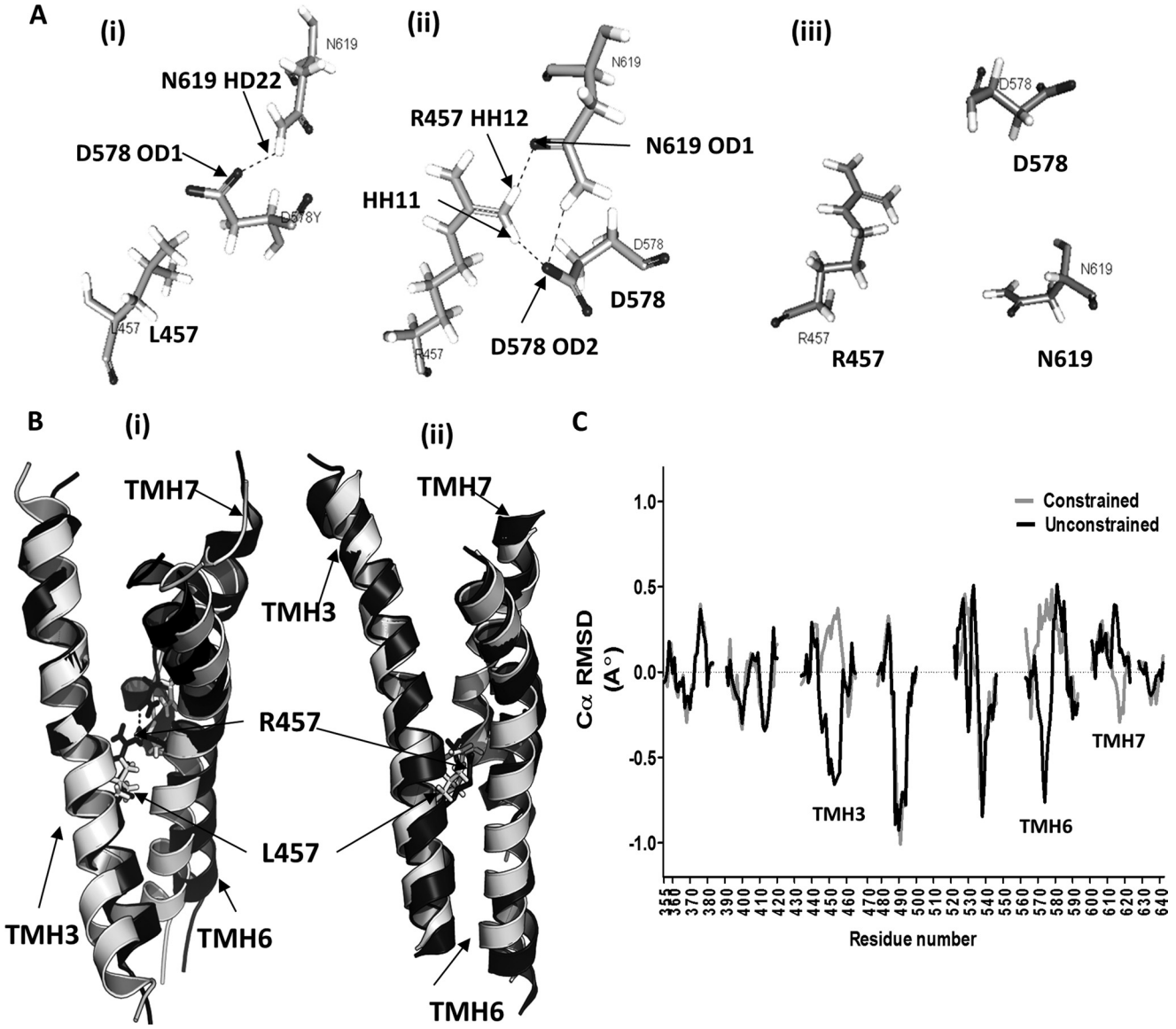

FIGURE 11. **Computational analysis of the mechanism of action of the mini-TMD antibodies.** *A*, shown is relative spatial orientation of Leu-457, Asp-578, and Asn-619 (*Ai*) in the modeled LHR WT TMD, Arg-457, Asp-578, and Asn-619 in the modeled mutant LHR L457R (*Aii*), and Arg-457, Asp-578, and Asn-619 in ECL-juxtamembrane domain constrained LHR L457R mutant (*Aiii*), simulating binding of the mini-TMD antibodies. Hydrogen bonds are shown as *dotted lines*. *B*, MD simulations were carried on the modeled structures of the wild type and LHR457 mutants. TMH3, TMH6, and TMH7 derived from the MD-simulated model were superimposed on each other. Similar analysis was carried out by constraining the ECLs to simulate an antibody-bound condition. Shown are relative changes in the helix orientations of TMH3, TMH6, and TMH7 in the WT (shown as *white helices*) and LHR L457R mutant (*black helices*) (*Bi*) and the same shown in the mini-TMD antibody-bound-simulated condition (*Bii*). Changes in the positions of Leu-457 in WT and Arg-457 in mutant are shown as *white* and *black sticks*. *C*, Cα-backbone r.m.s.d. were calculated for all residues of the LHR L457R mutant with respect to the WT receptor after performing MD simulation on each model. *Gray lines* indicate MD simulations under constrained ECLs (mimicking antibody bound condition), whereas *black lines* indicate no constrain on the ECLs (simulating a free unbound receptor). r.m.s.d. calculations were not carried out for ECLs or ICLs and are marked by gaps in the plot. Reversal of the trajectory may be observed for TMH3, TMH6, and TMH7.

mutant was incorporated using MODELLER, and the side chain conformations were refined through the *ChiRotor* algorithm refinement. MD simulations were performed on the WT and mutant receptors under identical conditions, and the mean structure was extracted from a production run of the last 800 ps. The structural alignment of the WT and L457R-simulated structures reveal significant Cα deviations with the ICL2 tethers deviating by 6.7 Å, and the main chain r.m.s.d. for ECL 1 was found to be 3.8 Å (Fig. 11*B*). More interestingly, in the WT receptor the OD1 atom of Asp-578 was found to be hydrogen-bonded to HD22 atom of Asn-619, whereas in L457R this interaction was replaced by hydrogen bonding between the HH12 atom of Arg-457 and the OD1 atom of Asn-619 with an additional hydrogen bond between HH11 of Arg-457 with OD2 with Asp-578 (Fig. 11*A*). Mean side-chain movement for Asp-578 was found to be 2.3 Å, and this along with changes in ICL2 can explain the stabilization and high basal activity of the mutant receptor.

Simulation of antibody binding to the receptor exoloops was carried out by keeping the centroid of the ECLs under a relatively stiff harmonic potential (force constant 3000 piconewtons/Å) with the residues of the ECLs under a spring constant of 65 piconewtons. This setup allowed the TMD to adapt to the enforced antibody binding, *e.g.* by rotations, intramolecular

conformational motions, or as experienced during induced fit, as observed in typical antigen-antibody atomic force microscopy (AFM) experiments (39). MD simulations of the L457R mutant in the presence or absence of the above constraint yielded surprising results. Not only was the tripartite hydrogen bonding of the Arg-457, Asp-578, and Asn-619 lost, Arg-457 (Fig. 11*Aiii*) showed a negative trajectory where the helix 3 deviated 3.1 Å from the mean Cα of the unconstrained mutant model. A plot of all the Cα r.m.s.d. of the mean trajectory of TMH residues in the constrained and unconstrained mutant receptor using the unconstrained WT receptor as the reference showed a large reversal of the simulated trajectories (>1 Å) in TMH3 and TMH6 with smaller perturbations in the juxtamembranal regions of ECL2 and TMH5 and cytoplasmic face of ICL3 and TMH7 (Fig. 11*C*). The interhelical network of hydrogen bond between Leu-457, Asp-578, and Asn-619 has been shown to be highly conserved in all the three GpHR members as shown through the rearrangement of carboxylate oxygen of TSHR N674 (Asn-619 in LHR) with Asp-633 (Asp-578 in LHR), resulting in a switch between the activated and inactivated states (29). Control of such an interhelical molecular switch by modulating the ECLs has already been exploited in designing small molecule agonist for TSHR and LHR (19). The above data taken together would suggest that antibody or small molecules binding to ECLs or the exoplasmic face of the TMH can affect global TMD conformation.

Significance of the Mini-TMD Antibodies; Applicability as a Therapeutic Strategy or a Tool for Biophysical Studies of the TMD—Activating mutations in TSHR typically cause thyroid cancer and precocious puberty in the case of LHR. S281I and I486F are typical germ-line mutations that cause toxic adenomas, whereas I568T and V656F are somatic mutations that cause hot nodules and adenomas, respectively. L457R in LHR causes Leydig cell hyperplasia, and the corresponding mutation in TSHR (L512R) has been shown to be involved in thyroid nodule formation. Therapeutic strategies such as epidermal growth factor receptor (EGFR)-specific monoclonal antibody for cancer treatment are unavailable in such cases, and surgical removal of the thyroid or testis remains the sole alternative. This study has shown that antibodies against TMD can be the right therapeutic tools for these conditions.

In addition, the ability of the mini-TMD antibodies to stabilize TMHs offers a powerful tool for crystallography of GpHRs. Antibody fragments that recognize the native protein conformations have been shown to facilitate crystallization of other membrane proteins by increasing the polar surface area for protein-protein contacts and by restricting the flexibility of mobile domains. The mini-TMD antibodies seem to be an ideal tool for purification of the stabilized TMD.

In conclusion, we report a novel strategy of developing specific antibodies against the exoloops of GpHRs. We have used these antibodies to demonstrate the differential interactions of the HinR of LHR as compared with those of TSHR and FSHR. In addition, we have provided preliminary evidence of a possible cooperative translocation of the ECLs and the α-subunit into the hydrophobic core of TMH and provided a physical basis of the mechanism of ECL control of the TMHs. A theoretical model is presented to explain the inhibitory effect of the mini-TMD antibodies on hormone binding and basal activity of WT and mutant receptors.

Acknowledgments—We thank the University Grant Commission and Department of Science and Technology for infrastructure support. The TSHR/LHR chimeric construct (TSH-LHR-6) and LHR TMH3 activating mutant L457R were kind gifts of Prof. Basil Rapoport (Cedars-Sinai Medical Center, UCLA) and Prof. Deborah Segaloff (University of Iowa), respectively.

REFERENCES

1. Kristiansen, K. (2004) Molecular mechanisms of ligand binding, signaling, and regulation within the superfamily of G-protein-coupled receptors. Molecular modeling and mutagenesis approaches to receptor structure and function. *Pharmacol. Ther.* **103,** 21–80
2. Fan, Q. R., and Hendrickson, W. A. (2005) Structure of human follicle-stimulating hormone in complex with its receptor. *Nature* **433,** 269–277
3. Moyle, W. R., Campbell, R. K., Rao, S. N., Ayad, N. G., Bernard, M. P., Han, Y., and Wang, Y. (1995) Model of human chorionic gonadotropin and lutropin receptor interaction that explains signal transduction of the glycoprotein hormones. *J. Biol. Chem.* **270,** 20020–20031
4. Moyle, W. R., Xing, Y., Lin, W., Cao, D., Myers, R. V., Kerrigan, J. E., and Bernard, M. P. (2004) Model of glycoprotein hormone receptor ligand binding and signaling. *J. Biol. Chem.* **279,** 44442–44459
5. Moyle, W. R., Lin, W., Myers, R. V., Cao, D., Kerrigan, J. E., and Bernard, M. P. (2005) Models of glycoprotein hormone receptor interaction. *Endocrine* **26,** 189–205
6. Mueller, S., Jaeschke, H., Günther, R., and Paschke, R. (2010) The hinge region: an important receptor component for GPHR function. *Trends Endocrinol. Metab.* **21,** 111–122
7. Agrawal, G., and Dighe, R. R. (2009) Critical involvement of the hinge region of the follicle-stimulating hormone receptor in the activation of the receptor. *J. Biol. Chem.* **284,** 2636–2647
8. Neumann, S., Claus, M., and Paschke, R. (2005) Interactions between the extracellular domain and the extracellular loops as well as the 6th transmembrane domain are necessary for TSH receptor activation. *Eur. J. Endocrinol.* **152,** 625–634
9. Kleinau, G., Jaeschke, H., Mueller, S., Raaka, B. M., Neumann, S., Paschke, R., and Krause, G. (2008) Evidence for cooperative signal triggering at the extracellular loops of the TSH receptor. *FASEB J.* **22,** 2798–2808
10. Hicks, D., and Barnstable, C. J. (1987) Different rhodopsin monoclonal antibodies reveal different binding patterns on developing and adult rat retina. *J. Histochem. Cytochem* **35,** 1317–1328
11. Blanpain, C., Vanderwinden, J. M., Cihak, J., Wittamer, V., Le Poul, E., Issafras, H., Stangassinger, M., Vassart, G., Marullo, S., and Schlndorff, D. (2002) Multiple active states and oligomerization of CCR5 revealed by functional properties of monoclonal antibodies. *Mol. Biol. Cell* **13,** 723–737
12. Eswar, N., Webb, B., Marti-Renom, M. A., Madhusudhan, M., Eramian, D., Shen, M. Y., Pieper, U., and Sali, A. (2007) Comparative protein structure modeling using MODELLER. *Curr. Protoc. Protein Sci.*, Chapter 2, Unit 2.9
13. Worth, C. L., Kleinau, G., and Krause, G. (2009) Comparative sequence and structural analyses of G-protein-coupled receptor crystal structures and implications for molecular models. *PLoS ONE* **4,** e7011
14. Hildebrand, P. W., Goede, A., Bauer, R. A., Gruening, B., Ismer, J., Michalsky, E., and Preissner, R. (2009) SuperLooper. A prediction server for the modeling of loops in globular and membrane proteins. *Nucleic Acids Res.* **37,** W571–W574
15. Canutescu, A. A., and Dunbrack, R. L., Jr. (2003) Cyclic coordinate descent. A robotics algorithm for protein loop closure. *Protein Sci.* **12,** 963–972
16. Spassov, V. Z., Flook, P. K., and Yan, L. (2008) LOOPER. A molecular mechanics-based algorithm for protein loop prediction. *Protein Eng. Des. Sel.* **21,** 91–100
17. Lee, B., Sharron, M., Blanpain, C., Doranz, B. J., Vakili, J., Setoh, P., Berg, E.,

Liu, G., Guy, H. R., Durell, S. R., Parmentier, M., Chang, C. N., Price, K., Tsang, M., and Doms, R. W. (1999) Epitope mapping of CCR5 reveals multiple conformational states and distinct but overlapping structures involved in chemokine and coreceptor function. *J. Biol. Chem.* **274,** 9617–9626

18. Yeagle, P. L., Alderfer, J. L., and Albert, A. D. (1997) Three-dimensional structure of the cytoplasmic face of the G protein receptor rhodopsin. *Biochemistry* **36,** 9649–9654
19. Neumann, S., Huang, W., Titus, S., Krause, G., Kleinau, G., Alberobello, A. T., Zheng, W., Southall, N. T., Inglese, J., Austin, C. P., Celi, F. S., Gavrilova, O., Thomas, C. J., Raaka, B. M., and Gershengorn, M. C. (2009) Small-molecule agonists for the thyrotropin receptor stimulate thyroid function in human thyrocytes and mice. *Proc. Natl. Acad. Sci. U.S.A.* **106,** 12471–12476
20. Brooks, B. R., Brooks, C. L., 3rd, Mackerell, A. D., Jr., Nilsson, L., Petrella, R. J., Roux, B., Won, Y., Archontis, G., Bartels, C., Boresch, S., Caflisch, A., Caves, L., Cui, Q., Dinner, A. R., Feig, M., Fischer, S., Gao, J., Hodoscek, M., Im, W., Kuczera, K., Lazaridis, T., Ma, J., Ovchinnikov, V., Paci, E., Pastor, R. W., Post, C. B., Pu, J. Z., Schaefer, M., Tidor, B., Venable, R. M., Woodcock, H. L., Wu, X., Yang, W., York, D. M., and Karplus, M. (2009) CHARMM. The biomolecular simulation program. *J. Comput. Chem.* **30,** 1545–1614
21. Roy, A., Kucukural, A., and Zhang, Y. (2010) I-TASSER. A unified platform for automated protein structure and function prediction. *Nat. Protoc.* **5,** 725–738
22. Heinig, M., and Frishman, D. (2004) STRIDE. A web server for secondary structure assignment from known atomic coordinates of proteins. *Nucleic Acids Res.* **32,** W500–W502
23. Rydzanicz, R., Zhao, X. S., and Johnson, P. E. (2005) Assembly PCR oligo maker. A tool for designing oligodeoxynucleotides for constructing long DNA molecules for RNA production. *Nucleic Acids Res.* **33,** W521-W525
24. Majumdar, R., and Dighe, R. R. (2012) The hinge region of human thyroid-stimulating hormone (TSH) receptor operates as a tunable switch between hormone binding and receptor activation. *PLoS ONE* **7,** e40291
25. Majumdar, R., Railkar, R., and Dighe, R. R. (2012) Insights into differential modulation of receptor function by hinge region using novel agonistic lutropin receptor and inverse agonistic thyrotropin receptor antibodies. *FEBS Lett.* **586,** 810–817
26. Wang, W., and Malcolm, B. A. (2002) Two-stage polymerase chain reaction protocol allowing introduction of multiple mutations, deletions, and insertions using QuikChange site-directed mutagenesis. *Methods Mol. Biol.* **182,** 37–43
27. Dighe, R. R., and Moudgal, N. R. (1983) Use of α- and β-subunit specific antibodies in studying interaction of hCG with Leydig cell receptors. *Arch. Biochem. Biophys.* **225,** 490–499
28. Saha, S., Majumdar, R., Dighe, R. R., and Chakravarty, A. R. (2010) Enhanced photodynamic effect of cobalt(III) dipyridophenazine complex on thyrotropin receptor expressing HEK293 cells. *Metallomics* **2,** 754–765
29. Neumann, S., Krause, G., Chey, S., and Paschke, R. (2001) A free carboxylate oxygen in the side chain of position 674 in transmembrane domain 7 is necessary for TSH receptor activation. *Mol. Endocrinol.* **15,** 1294–1305
30. Claus, M., Jaeschke, H., Kleinau, G., Neumann, S., Krause, G., and Paschke, R. (2005) A hydrophobic cluster in the center of the third extracellular loop is important for thyrotropin receptor signaling. *Endocrinology* **146,** 5197–5203
31. Bulheller, B. M., and Hirst, J. D. (2009) DichroCalc. Circular and linear dichroism online. *Bioinformatics* **25,** 539–540
32. Kleinau, G., Claus, M., Jaeschke, H., Mueller, S., Neumann, S., Paschke, R., and Krause, G. (2007) Contacts between extracellular loop two and transmembrane helix six determine basal activity of the thyroid-stimulating hormone receptor. *J. Biol. Chem.* **282,** 518–525
33. Zeng, H., Phang, T., Song, Y. S., Ji, I., and Ji, T. H. (2001) The role of the hinge region of the luteinizing hormone receptor in hormone interaction and signal generation. *J. Biol. Chem.* **276,** 3451–3458
34. Nishi, S., Nakabayashi, K., Kobilka, B., and Hsueh, A. J. (2002) The ectodomain of the luteinizing hormone receptor interacts with exoloop 2 to constrain the transmembrane region. Studies using chimeric human and fly receptors. *J. Biol. Chem.* **277,** 3958–3964
35. Zhang, M., Tong, K. P., Fremont, V., Chen, J., Narayan, P., Puett, D., Weintraub, B. D., and Szkudlinski, M. W. (2000) The extracellular domain suppresses constitutive activity of the transmembrane domain of the human TSH receptor. Implications for hormone-receptor interaction and antagonist design. *Endocrinology* **141,** 3514–3517
36. Nurwakagari, P., Breit, A., Hess, C., Salman-Livny, H., Ben-Menahem, D., and Gudermann, T. (2007) A conformational contribution of the luteinizing hormone-receptor ectodomain to receptor activation. *J. Mol. Endocrinol.* **38,** 259–275
37. Ho, S. C., Van Sande, J., Lefort, A., Vassart, G., and Costagliola, S. (2001) Effects of mutations involving the highly conserved S281HCC motif in the extracellular domain of the thyrotropin (TSH) receptor on TSH binding and constitutive activity. *Endocrinology* **142,** 2760–2767
38. Wonerow, P., Neumann, S., Gudermann, T., and Paschke, R. (2001) Thyrotropin receptor mutations as a tool to understand thyrotropin receptor action. *J. Mol. Med.* **79,** 707–721
39. Heymann, B., and Grubmüller, H. (2001) Molecular dynamics force probe simulations of antibody/antigen unbinding. entropic control and nonadditivity of unbinding forces. *Biophys. J.* **81,** 1295–1313
40. Gadkari, R. A., Sandhya, S., Sowdhamini, R., and Dighe, R. R. (2007) The antigen binding sites of various hCG monoclonal antibodies show homology to different domains of LH receptor. *Mol. Cell. Endocrinol.* **260,** 23–32
41. Yoo, J., Zeng, H., Ji, I., Murdoch, W. J., and Ji, T. H. (1993) COOH-terminal amino acids of the α subunit play common and different roles in human choriogonadotropin and follitropin. *J. Biol. Chem.* **268,** 13034–13042
42. Shinozaki, H., Fanelli, F., Liu, X., Jaquette, J., Nakamura, K., and Segaloff, D. L. (2001) Pleiotropic effects of substitutions of a highly conserved leucine in transmembrane helix III of the human lutropin/choriogonadotropin receptor with respect to constitutive activation and hormone responsiveness. *Mol. Endocrinol.* **15,** 972–984
43. Kaneshige, M., Haraguchi, K., Endo, T., Anzai, E., and Onaya, T. (1995) The functional significance of the second extracellular loop of thyrotropin receptor in thyrotropin- and thyroid stimulating antibody-dependent signal transduction. *Horm. Metabol. Res.* **27,** 267–271
44. Dupakuntla, M., and Mahale, S. D. (2010) Accessibility of the extracellular loops of follicle stimulating hormone receptor and their role in hormone-receptor interaction. *Mol. Cell. Endocrinol.* **315,** 131–137
45. Gustavsson, B., Westermark, B., and Heldin, N. E. (1994) Point mutations of the thyrotropin receptor determining structural requirements for its ability to bind thyrotropin and to stimulate adenylate cyclase activity. *Biochem. Biophys. Res. Commun.* **199,** 612–618
46. Kosugi, S., Matsuda, A., Hai, N., Aoki, N., Sugawa, H., and Mori, T. (1997) Aspartate-474 in the first exoplasmic loop of the thyrotropin receptor is crucial for receptor activation. *FEBS Lett.* **406,** 139–141
47. Szkudlinski, M. W., Fremont, V., Ronin, C., and Weintraub, B. D. (2002) Thyroid-stimulating hormone and thyroid-stimulating hormone receptor structure-function relationships. *Physiol. Rev.* **82,** 473–502
48. Van Sande, J., Massart, C., Costagliola, S., Allgeier, A., Cetani, F., Vassart, G., and Dumont, J. E. (1996) Specific activation of the thyrotropin receptor by trypsin. *Mol. Cell. Endocrinol.* **119,** 161–168
49. Vlaeminck-Guillem, V., Ho, S. C., Rodien, P., Vassart, G., and Costagliola, S. (2002) Activation of the cAMP pathway by the TSH receptor involves switching of the ectodomain from a tethered inverse agonist to an agonist. *Mol. Endocrinol.* **16,** 736–746
50. Mizutori, Y., Chen, C. R., McLachlan, S. M., and Rapoport, B. (2008) The thyrotropin receptor hinge region is not simply a scaffold for the leucine-rich domain but contributes to ligand binding and signal transduction. *Mol. Endocrinol.* **22,** 1171–1182
51. Kleinau, G., Jäschke, H., Neumann, S., Lättig, J., Paschke, R., and Krause, G. (2004) Identification of a novel epitope in the thyroid-stimulating hormone receptor ectodomain acting as intramolecular signaling interface. *J. Biol. Chem.* **279,** 51590–51600
52. Jaeschke, H., Neumann, S., Kleinau, G., Mueller, S., Claus, M., Krause, G., and Paschke, R. (2006) An aromatic environment in the vicinity of serine 281 is a structural requirement for thyrotropin receptor function. *Endocrinology* **147,** 1753–1760